


Lithological and Chemical Constraints on the Mount Freda-Evening Star Mineral System, Cloncurry District Improve IOCG Metal Source Targeting

**Professor Ken Collerson
PhD., FAusIMM**

**KDC Consulting
ABN 44 584 455 091
Brisbane, Queensland**



June 25th 2019




TABLE OF CONTENTS

EXECUTIVE SUMMARY	2
1 INTRODUCTION	6
2 BACKGROUND	6
3 MOUNT FREDA - EVENING STAR MINERAL SYSTEM	8
3.1 Background	8
3.2 Lithological Review of Evening Star Cores	13
3.2.1 Pyroxenite dykes	13
3.2.2 Potassium Fenites	16
4. ES19-DD001 AND ES19-DD003 ASSAYS	22
4.1 The Tuffisite Breccia System	22
4.1.1 Chemical Comparison	22
4.1.2 Transition Elements	25
4.1.3 Scandium	25
4.1.4 Rare Earth Systematics	26
4.1.5 La/Yb versus Total Rare Earth Discrimination Projection	27
4.1.6 CHARAC Ratio Systematics	28
4.1.8 Constraints from Primitive Mantle Normalised Ta/U and Nb/Th ratios	30
4.1.9 Gold Tellurium and Bismuth	31
4.1.10 Molar Cu/Au Systematics and Metal Sources	32
5. SUMMARY AND CONCLUSIONS	37
6. RECOMMENDATIONS	41
7. REFERENCES CITED	42
8. PEER REVIEW	46
9. CERTIFICATE OF QUALIFIED PERSON	47

Executive Summary

The discovery of a copper, gold, nickel and cobalt - rich tuffisite breccia pipe in two diamond drill cores (ES19DD001 and ES19DD003) at Ausmex Evening Star prospect has significant implications for the Cloncurry District IOCG mineral system model and thus, for exploration strategies and target identification.

Tuffisite is a matrix supported heterolithic intrusive pyroclastic breccia that forms in hydrothermal gas/fluid streams that advance ahead of ascending columns of magma. Although similar in appearance pyroclastic tuffs (volcanic ash deposits), relationships in the core show that the lithology is intrusive in origin.

Similar pyrite-bearing pebble breccia dykes cutting magmatic hydrothermal intrusion breccias occur at the Ladolam gold mine on Lihir in PNG (Muller and Groves, 2018). Hydrothermal breccias associated with tuffisite dykes have also been reported occur at the giant Oyo Tolgoi Cu-Au-Mo deposit in Mongolia (Porter 2016).

The presence of a tuffisite pipe in the Evening Star - Mount Freda prospect indicates a close proximity to the magmatic metal source that produced epithermal high-grade gold mineralisation at Mount Freda and also in Ausmex Golden Mile exploration area.

Uniformity of rare earth profiles, over an 8.5 m wide brecciated core interval, indicates that tuffisite pipe formation involved a very-high fluid/rock ratio and efficient mixing. Chemistry of the core shows that the fluid was fluorine, tellurium and sulphur rich, allowing the transport of Au, Ag, Cu, Ni and Co etc derived from a **deeper large alkaline IOCG or porphyry source.**

Identification of tuffisite was based initially on structure and textural relationships in the DD001 core. It was subsequently recognised in DD003, where it cuts crackle brecciated quartzite.

In DD001, the metal-rich tuffisitic breccia pipe occurs between 80 to 88.5 m. In DD003, the brecciated unit is deeper (between 159.52 and 163 m). As the breccia is narrower in DD003 (3.48 m), it is likely to be a plunging diatreme-like intrusion, originating from a large deeper, mineral-rich source.

A 3.6 m wide interval comprising native copper bearing gossan at a shallower depth in DD001 (59.5-63 m) was provisionally interpreted to related to the tuffisite identified between 80 and 88.5 m. Assays confirmed this interpretation.

From the orientation of the core, the tuffisite pipe is inferred to plunge towards the east, in the direction of the large magnetic anomaly Ausmex shares with Newcrest Mining Limited.

This south east - north west vector is consistent with the interpretation that the tuffisite pipe acted as a conduit for hydrothermal fluids that generated the gold-rich epithermal mineral system at Mount Freda. The link between the tuffisite brecciation and epithermal processes is supported by epithermal colloform banded silica - rich veins and quartz vughs that cut units of tuffisite.

Assays from DD001 and DD003 confirm the metallogenic significance of the tuffisite breccia system.

Tuffisite breccias in DD001 and DD003 cores have significant metal contents, e.g., copper (1060 to 9640 ppm; average 8420 ± 3321 and 3290 to 21,700 (2.17%) ppm; average 8530 ± 7612 ppm), gold (0.03 to 0.69 g/t; average 0.36 ± 0.18 g/t and 0.19 to 3.36 g/t; average 1.29 ± 1.79 g/t), nickel (107 to 599 ppm; average 339 ± 121 ppm and 92 to 309 ppm; average 233 ± 105 ppm), cobalt (124.5 to 496 ppm; average 295 ± 98 ppm and 82.6 to 222 ppm; average 192 ± 70 ppm) and molybdenum (3.29 to 12.7 ppm; average 6.63 ± 3.37 ppm and 3.84 to 11.1 ppm; average 5.26 ± 1.36 ppm).

The tuffisite also contains anomalous bismuth, sulphur and tellurium e.g., bismuth (0.07 to 2.52 ppm; average 0.80 ± 0.89 and 0.28 to 1.24 ppm; average 0.64 ± 0.52 ppm), sulphur (2.8 to 10 wt.%; average 8.2 ± 2.2 and 3.25 to 6.43 wt. %; average 5.6 ± 1.4 wt. %) and tellurium (3.29 to 12.7 ppm; average 6.63 ± 3.37 and 0.7 to 3 ppm; average 0.64 ± 0.52 ppm).

The native Cu and gossanous unit in DD001 exhibits similar **or even more extreme levels of enrichment**, e.g., copper (1.03 to 4.32 wt. %; average 2.65 ± 1.37 wt. %) gold (0.33 to 2.07g/t; average 1.08 ± 0.64 g/t), nickel (443 to 1100 ppm; average 723 ± 251 ppm), cobalt (177 to 881 ppm; average 508 ± 314 ppm) and molybdenum (8.75 to 70.4 ppm; average 32 ± 23.8 ppm). This unit also contains anomalous bismuth, sulphur and tellurium e.g., bismuth (0.43 to 1.73 ppm; average 0.93 ± 0.51 ppm), sulphur (5.7 to 10 wt.%; average 9.1 ± 1.9 wt.%) and tellurium (3.42 to 7.46 ppm; average 5.1 ± 1.7 ppm).

When compared to the mean composition of 155 assays of Soldiers Cap Group host rocks in DD001, the tuffisite and gossanous unit are clearly anomalous. For example, copper (553 ± 1075 ppm), gold (0.02 to 0.06 g/t), nickel (90 ± 114 ppm), cobalt (102 ± 135 ppm), molybdenum (2.26 ± 3.14 ppm), bismuth (0.11 ± 0.22 ppm), sulphur (1.14 ± 2.33 wt.%) and tellurium (0.29 ± 0.62 ppm).

Other key findings are as follows;

(1) The elements association (Cu - Co - Ni - Au with Sc and Te) in the tuffisite and Cu-rich gossan at Evening Star indicates derivation of the mineral system from an ultramafic - mafic source. The discovery of Fe-rich pyroxenite dykes in ES19DD001 and ES19DD003 core provides a link with this mantle source.

(2) Molar Cu/Au ratios <100,000 are also consistent with derivation of metals from an alkaline ultramafic (plume), **potentially a large porphyry** source as suggested by Collerson (2019).

(3) Pyroxenites, carbonate-rich mela-gabbros and alkali syenites, possibly associated with carbonatite, are present as dykes. The dykes have discordant contacts to fabrics in the host quartzites and have apophyses that cut the country rock fabrics at a high angle. These discordant relationships indicate that emplacement of the pyroxenites and mela-gabbros post-dated regional deformation associated with the Isan Orogeny at 1600 and 1580 Ma (Giles et al., 2006).

(4) Pyroxenite dykes and narrow carbonate veins are intimately associated with zones of potassium feldspar and locally magnetite, crystallisation. These lithologies are interpreted as potassic fenites. They clearly overprint and destroy metamorphic fabrics in the country rock Mount Norna Quartzite.

(5) The presence of widespread K and Fe alteration indicates a close proximal relationship of these cores to the source of the metasomatizing fluids (Potentially a large porphyry mineralised system at depth).

Importantly, these metasomatic textures are similar to microstructures reported from South Australian IOCGs (e.g., Prominent Hill, Schlegel and Heinrich, 2015; Schlegel et al., 2018).

(6) The magnetic anomaly that Ausmex shares with Newcrest Mining Limited at the adjacent Canteen IOCG target is provisionally interpreted to be a volatile-rich post-tectonic alkaline ultramafic to mafic intrusion that is capped by a metal-rich epithermal system.

(7) The epithermal system crops out along the Golden Mile, between Evening Star and Gilded Rose. The presence of this Au-rich epithermal zone reflects mineral deposition at a shallow crustal depth (<1,000 m) from magmatically derived hot-spring fluids that emanated from a deeper igneous source.

(8) Zones of sulphide-rich and carbonate-rich tuffisites identified at different depths in ES019 - DD001 and DD003 are important in this regard. Tuffisitic lithologies are common in alkaline complexes (Rosatelli et al., 2010), and also in Au-bearing

hydrothermal systems (Williams et al., 2000). **Thus, the tuffisites in the Evening Star core, could represent the pipe-like brecciated conduits that served as a channels for epithermal fluid and metal transport.**

(9) In chondrite normalised REE plots, the tuffisites in ES19 DD001 and ES19 DD003 yield identical pattern shapes with negative Eu and variable Y/Ho ratios that indicate the effect of F-fractionation. This is significant because F is an important ligand for metal transport in hydrothermal systems.

(10) In primitive mantle normalised Ta/U and Nb/Th plots, data for samples core >95 m in ES19 DD001 plot with ratios of ~1, indicating a strong lower mantle component. Ta/U_N and Nb/Th_N values for the tuffisite and gossan lie on a vector towards Ta/U_N and Nb/Th_N ratios that approach values of 0.001. **This vector is similar to that exhibited by Cu and Au rich alkaline porphyry systems. This suggests a possible link between the magmatic source of metals in IOCG deposits and in porphyry Au-Cu systems.** This source involves a mantle plume component, which provide Au and PGEs as well as heat for melting, and supra-subduction zone mantle wedge component, that has been enriched in Cu by fluids during slab dehydration.

(11) A volatile-rich post-tectonic alkaline ultramafic to mafic igneous composition thus provides an appropriate source of the poly-metallic element association (Au-Cu-Co-Ni-Sc-Pt-Pd-Re-Mo-REE-U-Th) reported from the IOCG mineral systems in the Cloncurry District.

(12) The presence of pyroxenites could explain the elevated Sc values reported from the Mt Freda - Evening Star mineral system.

Results of this investigation have significant implications for IOCG exploration and hence exploration strategies in the region.

These new data support for the mineral system model presented in ASX Release 29th February.

1 Introduction

This report was commissioned by Ausmex to investigate lithologies recovered in diamond drill cores (ES19DD001 and ES19DD003) during their current drilling campaign at the Mount Freda - Evening Star project, SE of Cloncurry.

Rationale for the investigation was to:

- Understand the origin and significance of the Canteen magnetic anomaly,
- Improve the mineral system model
- Comment on the prospectivity of the region

This report initially focuses on the interpretation of lithological observations.

Subsequent to the site visit, assay data for ES19DD001 and ES19DD003 were provided. The scope of the report was thus extended to include a discussion of the chemistry and metallogenic significance of sulphide-rich tuffsite lithologies identified at different depths in both cores.

2 Background

In exploration, key uncertainties in targeting mineralisation are knowledge of the metals source, the source of fluids and metal transport mechanism and the structural control deposition. Such mineral system information is critical to understand the origin of the Mesoproterozoic IOCG (iron oxide - copper - gold) deposits in the Eastern Succession of the Mount Isa Block.

The metal endowment of this area is interpreted to reflect the interplay of number of metallogenic/geodynamic events. These include continental back-arc rifting, regional metamorphic events associated with the Isan Orogeny and plume related alkaline magmatism. Although the role of plume magmatism was suggested for deposits in the adjacent Mary Kathleen Belt (Oliver, *et al.*, 1991), scant lithological or geochemical evidence was provided to support this hypothesis.

In a very innovative yet provocative paper, Groves and Vielreicher (2001) suggested that the end-member of the Olympic Dam-type IOCG systems were Si -poor volatile-rich alkaline magmas that were enriched in REEs, F, U, and Th could be. This is important in the context of the current study, as these magmas liberate sulphur-deficient volatiles that are enriched in Cu and Au (as well as other elements). They form phreatic breccia pipes and are also associated with extensive metasomatism. Furthermore, the multi-element association (Cu-Ni-V-Sc-PGEs-Au-Ag-Mo-Re) in many Cloncurry area IOCG deposits clearly requires an ultramafic to mafic alkaline source.

The recent discovery of alkaline ultramafic lithologies at Mount Cobalt containing elevated Au-PGE-Sc-Co-Cu and a similar element associations in epithermal systems in the Cloncurry District (Collerson 2019) confirms the role of deep sourced plume magmatism in the generation of IOCG deposits in the district.

This hypothesis also supports the geodynamic model of Betts *et al.*, (2007, 2009) who suggested that a stationary upwelling mantle plume impacted the Gawler Craton, Curnamona Craton and Mount Isa Block during break-up of the supercontinent called Columbia during the Mesoproterozoic. This caused the eastern margin of Precambrian Australia to separate from western Laurentia.

The alignment of alkaline intrusions that define a Mesoproterozoic plume track supports this hypothesis. Plume generated magmatism associated with this event, includes intrusions responsible for Olympic Dam mineralization at 1.59 Ga (e.g., Jagodinski, 2005 & 2014; Jagodinski *et al.*, 2016; Cherry *et al.*, 2018), the cryptic record of alkaline magmatism in the Mary Kathleen Belt and Eastern Succession of the Mount Isa Block at ~1.55 -1.5 Ga (Duncan *et al.*, 2011; Spandler *et al.*, 2016;

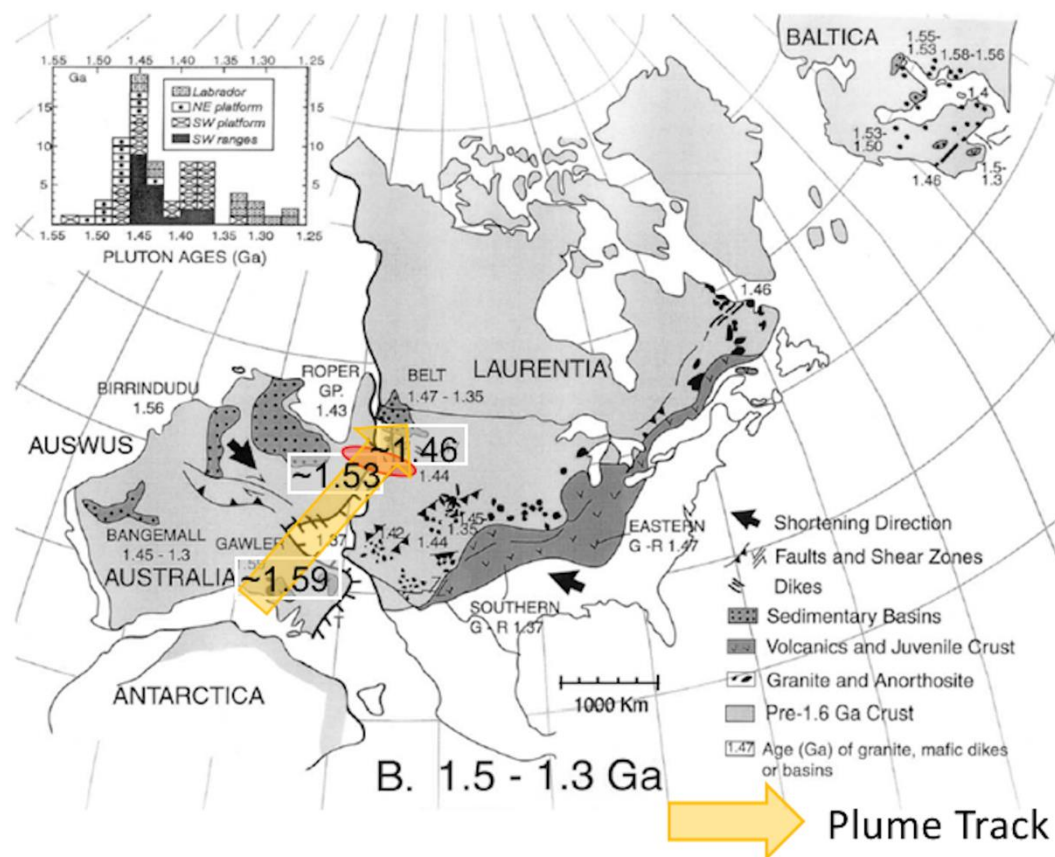


Figure 1: Reconstruction of Australia and Laurentia at 1.5 to 1.3 Ga. The pale orange arrow shows the trace of a plume track (Betts *et al.*, 2007; 2009). The pink oval shows the approximate position of the Idaho Cobalt Belt in Laurentia and the location of Co systems in the Mount Isa Block. Timing of alkaline magmatism in the Mt Isa Block (U-Pb titanite) and in Idaho (U-Pb xenotime; Aleinikoff *et al.*, 2015).

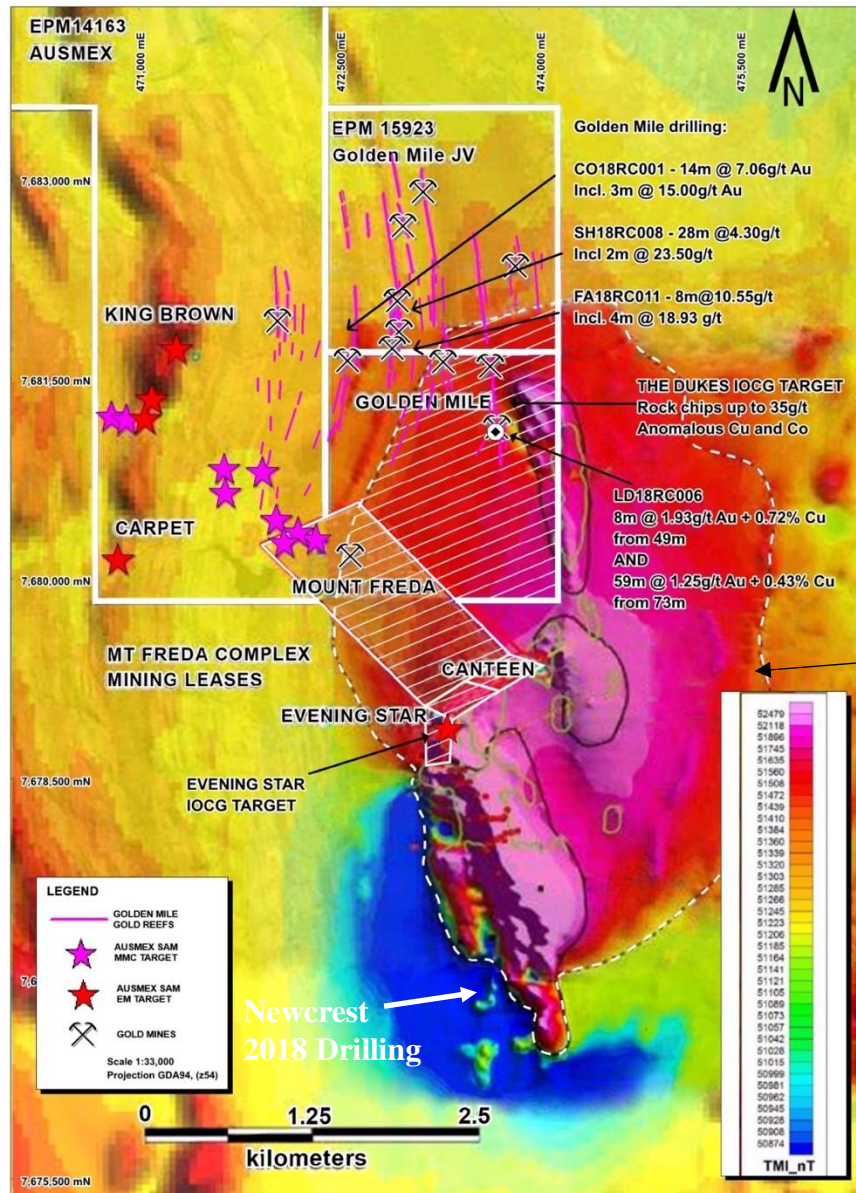
Collerson 2018) and a bi-modal suite of A-type granites and meta-gabbros in Idaho Cobalt Belt between 1.46 Ga (Aleinikoff et al., 2012; 2015) and 1370 to 1349 Ma (Saintilan et al., 2017).

3 Mount Freda - Evening Star Mineral System

3.1 Background

The Mount Freda and Evening Star project, is located proximal to a number of significant IOCG deposits in the Eastern Succession, Rocklands, Starra, Mount Elliot, SWAN, Mount Dore and Mount Freda. (Collerson, 2019). All of these systems display a characteristic poly-metallic association of Cu-Au-Ag-Mo and Re (Duncan *et al.*, 2014). The same association is also seen in mineral systems between Gilded Rose to Mount Freda and Evening Star, as well as at Mount Cobalt, further to the south (Collerson, 2019).

Location of the Mount Freda and Evening Star deposits are shown in Figure 2.



Massive Tier 1 IOCG Target previously Identified by Exco in 2012, recently drilled by Newcrest.

Figure 2: Mt Freda Complex Location plan. Note the close proximity of the Golden Mile to the massive 3 km x 5 km Tier 1 IOCG target that Ausmex shares with Newcrest Mining Limited, (Ausmex controls 30% of the IOCG target) as well as much of the higher crustal level hydrothermal-epithermal system

Geochemical analysis by Collerson (2019) indicated that the high-grade Au (and PGEs) within the Mt Freda-Evening Star mineral system were transported by hydrothermal fluids derived from a deeper large inferred igneous intrusion, shown in Figure 2. These fluids generated hot spring epithermal deposits at the surface. (Refer to ASX releases on 30th August 2018, 10th September 2018, 8th & 26th October 2018, 9th & 15th November 2018, for Mt Freda Complex Exploration drilling results). Source: QLD Gov. Mt Isa TMI GSQ open file dataset Survey GSQ1029 & [Exco IOCG Roadshow release 2012](#).

Reconnaissance assay data reported by Collerson (2019) for chip samples collected from the Evening Star, Mount Freda and Iron Duke deposits are given in Table 1. Images of these samples are shown in Figures 3 to 5.

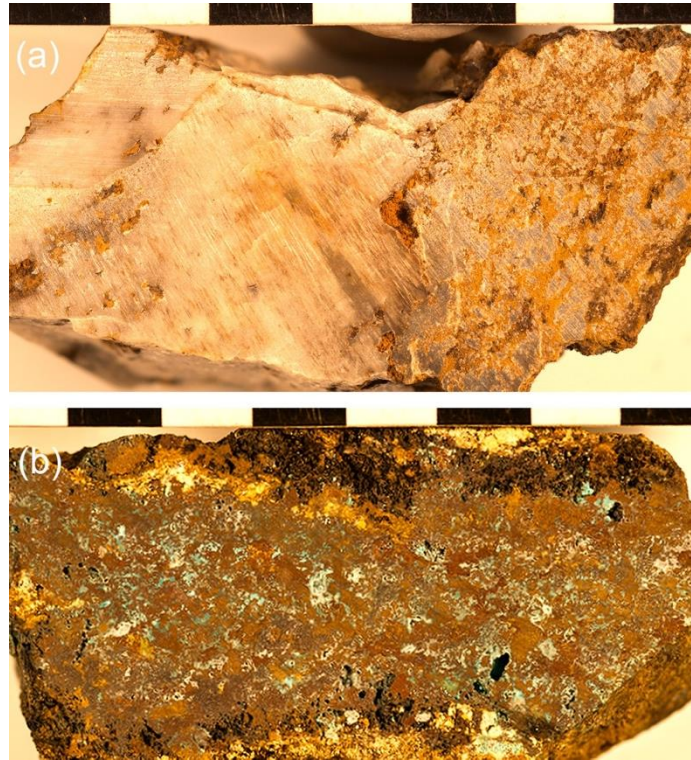


Figure 3: Evening Star (a) ES-1 Crackle brecciated quartz vein through coliform goethite and chlorite and (b) ES-2 Malachite-bearing iron-rich breccia. Scale bar intervals are 1 cm.

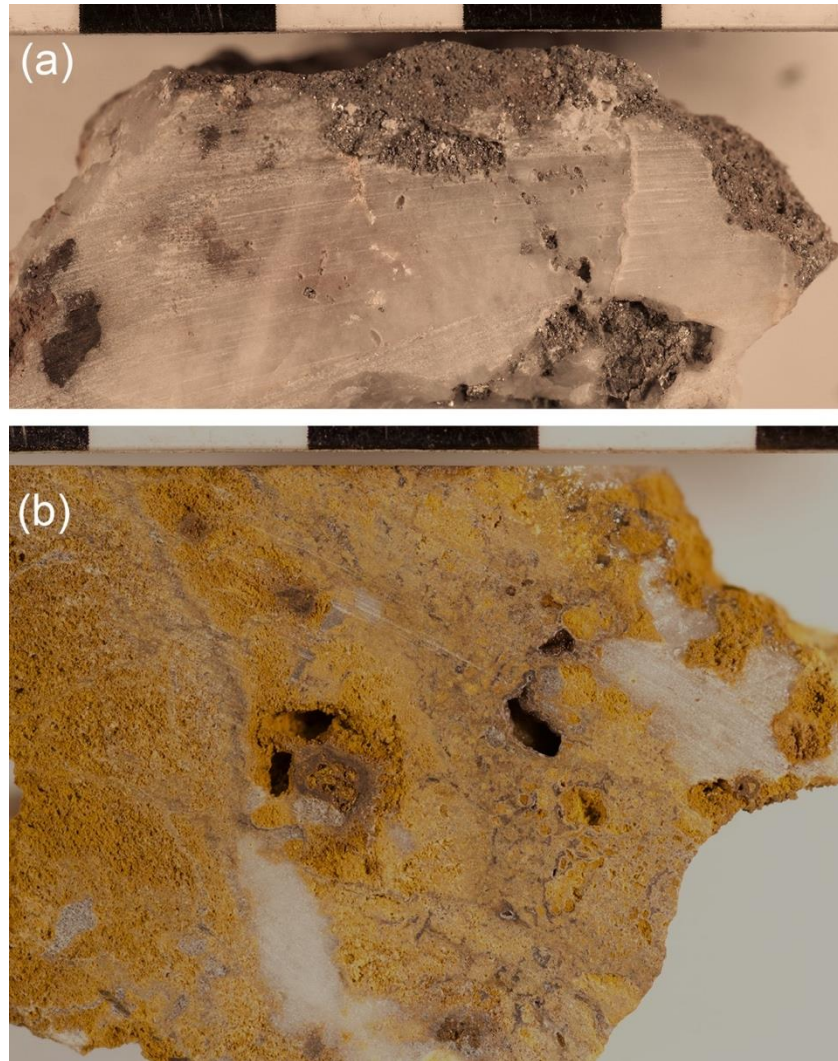


Figure 4: Mount Freda (a) MF-1 brecciated quartz with veins containing pyrrhotite - possible crackle breccia (b) MF-2 brecciated quartz with veins containing pyrrhotite - possible crackle breccia. Scale bar intervals are 1 cm.

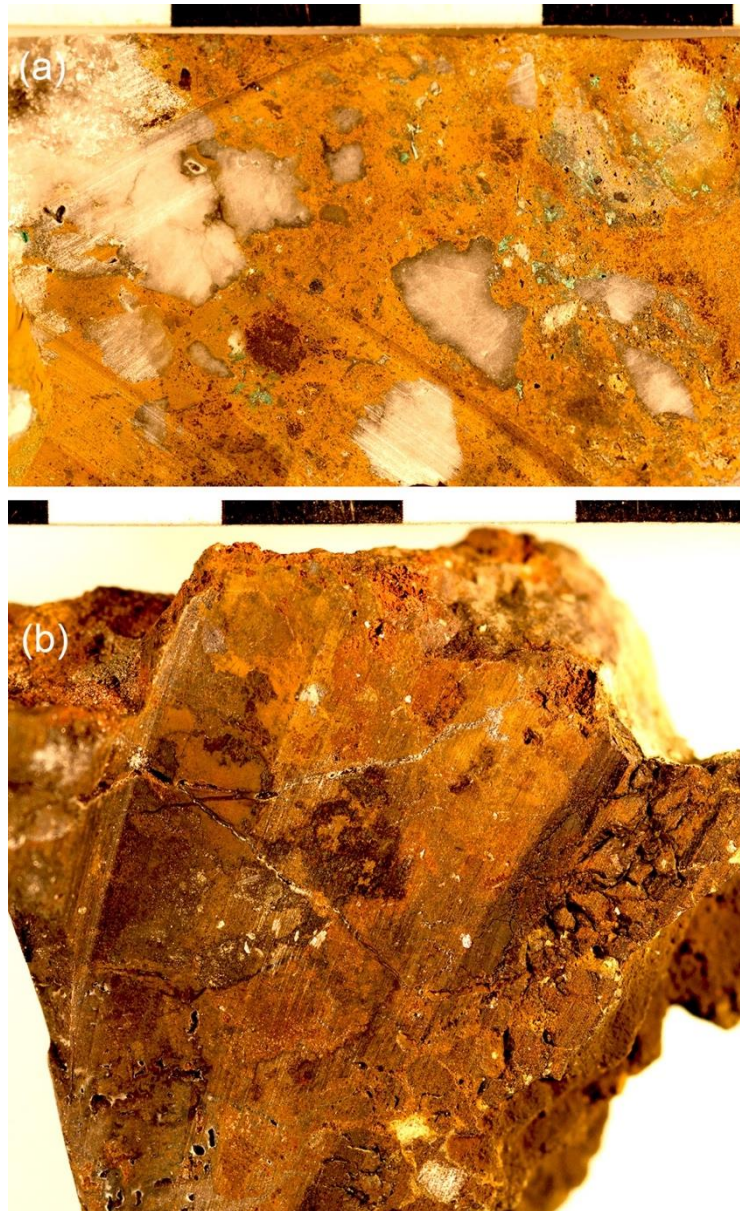


Figure 5: Iron Duke (a) ID-1 malachite-bearing iron-rich siliceous breccia and (b) ID-2 malachite-bearing iron-rich siliceous sulphide-bearing crackle breccia. Scale bar intervals are 1 cm.

Samples from Ausmex Mount Freda-Evening Star-Drillers Hut mineral system are significantly enriched in Sc, Co, F, Ni, Cu, Ni and Ag relative to Upper Crustal abundances (Table 1). They also show anomalism in Pd, Pt and Au. The low concentrations of Cu in Mt Freda, compared to Evening Star and Iron Duke is inferred to reflect the fact that Mount Freda is largely an epithermal system.

This enrichment in transition metals and precious metals strongly suggests supply of these elements from a mafic to ultramafic alkaline source, such as that discovered at Mount Cobalt (Collerson, 2019).

Table 1: Summary of Assay Data for Chip Samples

	Upper Crust*	Evening Star	Mount Freda	Iron Duke
Scandium	11 ppm	27 & 64 ppm	2 & 46.5 ppm	8.6 & 49.4 ppm
Fluorine		259 & 394 ppm	107 & 109 ppm	n.d.
Cobalt	10 ppm	140 & 170 ppm	608 & 969 ppm	150 & 1379 ppm
Copper	25 ppm	8 wt. %	70 & 169 ppm	1 & 4 wt. %
Nickel	20 ppm	240 & 360 ppm	52 & 70 ppm	35 & 524 ppm
Silver	50 ppb	0.3 & 0.5 ppm	0.9 & 1.4 ppm	2 & 9 ppm
Palladium	0.5 ppb	1.8 & 1.9 ppb	n.d.	0.7 & 1.7 ppb
Platinum		0.8 & 0.9 ppb	0.6 ppb	0.9 & 3.3 ppb
Gold	1.8 ppb	0.26 & 1.58 ppm	1.9 & 10 ppm	0.3 & 11 ppm

* From Taylor and McLelland (1995)

3.2 Lithological Review of Evening Star Cores

Cores from two drill holes ES19DD001 and ES19DD003 were examined in this study. The holes are located adjacent the large IOCG target called Canteen shown in Figure 2 that has recently been drilled by Newcrest Limited.

Key observations relevant to understanding the nature of the mineral system and thus the prospectivity of the tenement are reported below.

3.2.1 Pyroxenite dykes

Narrow coarse-grained pyroxenite dykes up to 20 cm in width occur at a number of depths in ES19-DD003. Examples are shown in Figures 6, 7 and 8. The pyroxenites are coarse to medium grained and are composed abundant dark green clinopyroxene which shows alteration to the prismatic secondary actinolite.

The dykes exhibit discordant contacts to fabrics in the host quartzites. Some dykes display apophyses that cut the country rock fabrics at a high angle. These relationships indicate that emplacement of the pyroxenite dykes post-dated regional deformation associated with the Isan Orogeny between 1600 and 1580 Ma (Giles et al., 2006).

Regional metamorphic fabrics next to the dykes are diffusely overprinted by zones of pink K-feldspar alteration which resembles fenitisation, a metasomatic process commonly associated with alkaline magmatism (Elliott et al., 2018). The presence of pyroxenites and associated "fenite" in the Evening Star core provides additional

constraints on origin of the multi-element IOCG systems in the Cloncurry area, suggesting an association with a volatile-rich ultramafic alkaline magma.

The presence of these pyroxenite dykes and associated fenites suggests proximity to an alkaline intrusion. This is most likely the Canteen geophysical target in the adjacent Newcrest JV which extends into the Ausmex tenement near Evening Star and Iron Duke (Figure 2).

The presence of pyroxenite also explains the elevated Sc values seen in the Mt Freda - Evening Star mineral system (Table 1). This is because pyroxene is a mineral into which Sc partitions (Williams-Jones & Vasyukova, 2018).

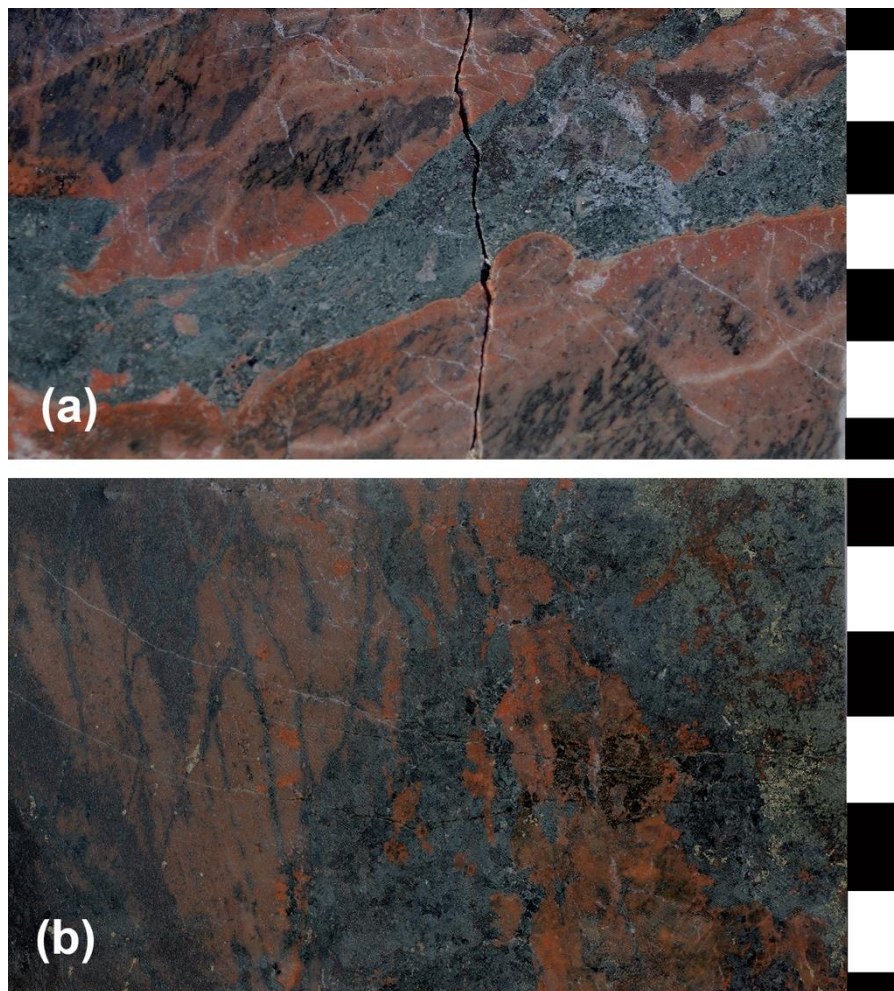


Figure 6: (a) Pyroxenite intrusion (dyke) cutting meta-mafic unit in core from ES19-DD003 at 44.85 m Shows extensive metasomatic alteration (fenitisation) that resulted in the crystallization of K-feldspar that obliterates metamorphic fabrics. This is typical of fenite. (b) Pyroxenite associated with K-fenite in ES19-DD003 at 13.2 - 13.4 m.

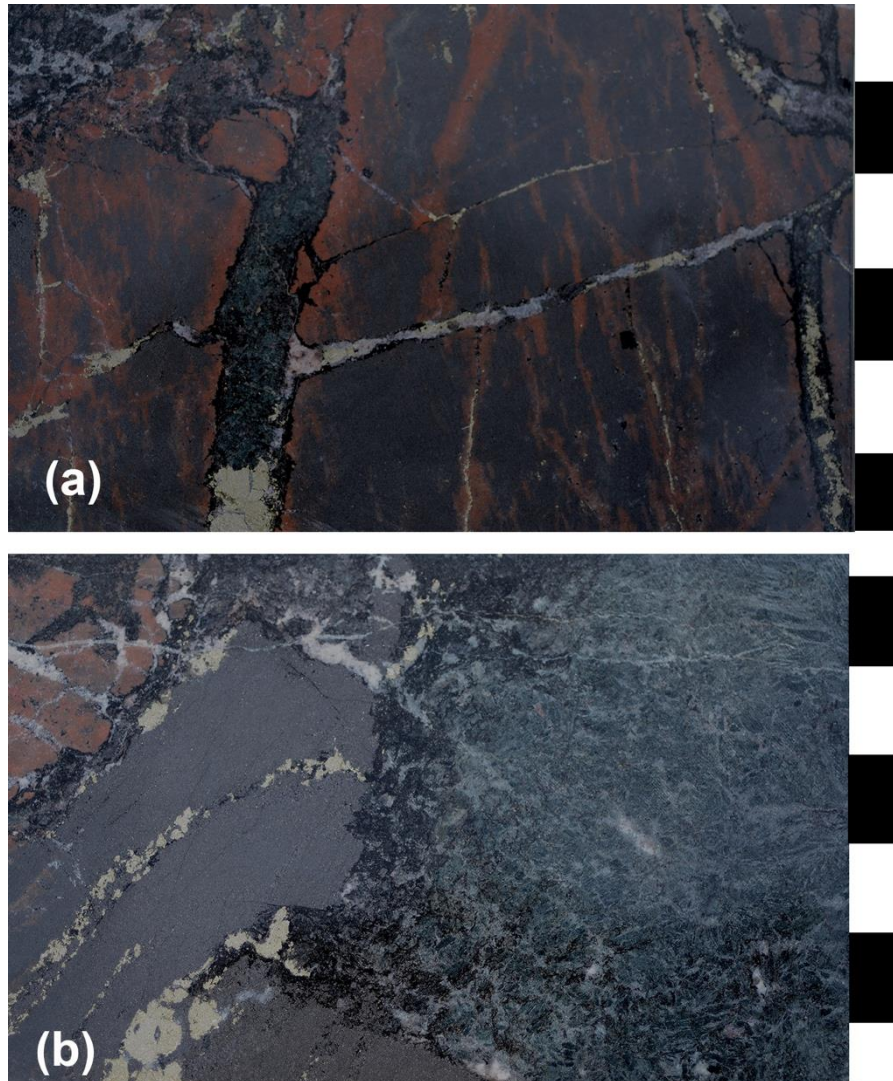


Figure 7: (a) Pyroxenite intrusion (dyke) cutting K-fenitised meta-mafic unit in core from ES19-DD003 at 31.2-31.4 m Shows extensive metasomatic alteration (fenitisation) that resulted in the crystallization of K-feldspar that obliterates metamorphic fabrics. This is typical of fenite. (b) Pyrite bearing pyroxenite dyke associated with K-fenite and magnetite in ES19-DD003 at 31.5 - 31.7 m. Narrow apophyses of pyroxenite cut the unit of magnetite and extend into the K-feldspar rich fenite (top left).

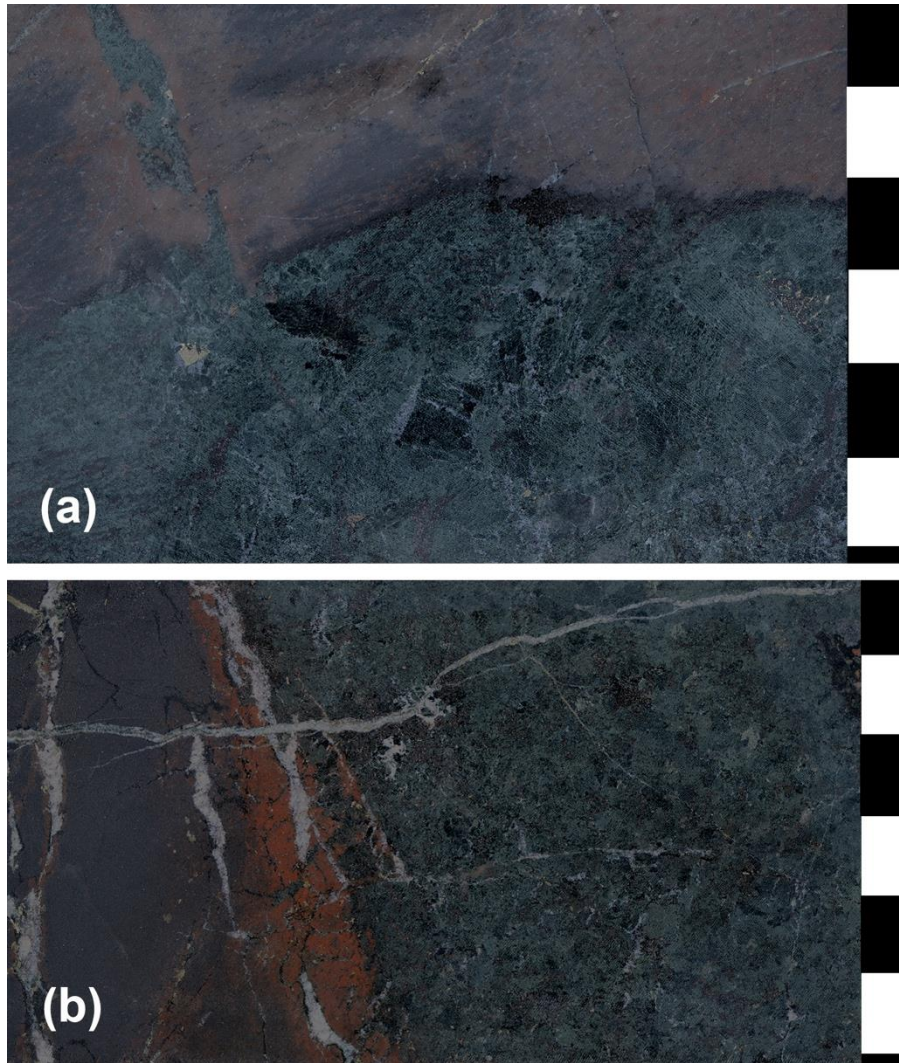


Figure 8: (a) Coarse grained pyroxenite intrusion (dyke) cutting K-fenitised meta-mafic unit in core from ES19-DD003 at 41.8 - 42m. Shows extensive metasomatic alteration (fenitisation) that resulted in the crystallization of K-feldspar that obliterates metamorphic fabrics. This is typical of fenite. (b) Pyrite bearing gabbroic to pyroxenite dyke associated K-fenite and magnetite crystallization in ES19-DD003 at 53.2 - 53.5 m.

3.2.2 Potassium Fenites

The pyroxenite dykes and narrow veins of carbonate are invariably associated with zones of potassium feldspar alteration that are interpreted as potassic fenites.

Fenite is a metasomatic alteration associated with carbonatite and alkaline intrusions. It is also caused by advanced CO₂ alteration (carbonation) of felsic and mafic lithologies. Such a process is called fenitisation.

These metasomatic fenite zones clearly overprint and destroy metamorphic fabrics in the Mount Norna Quartzite. Examples of fenite textures that also commonly associated with formation of crackle breccias are shown in Figure 9. It is noteworthy

that these textures are similar to textures reported from South Australian IOCGs at Prominent Hill (e.g., Schlegel and Heinrich, 2015; Schlegel et al., 2018).

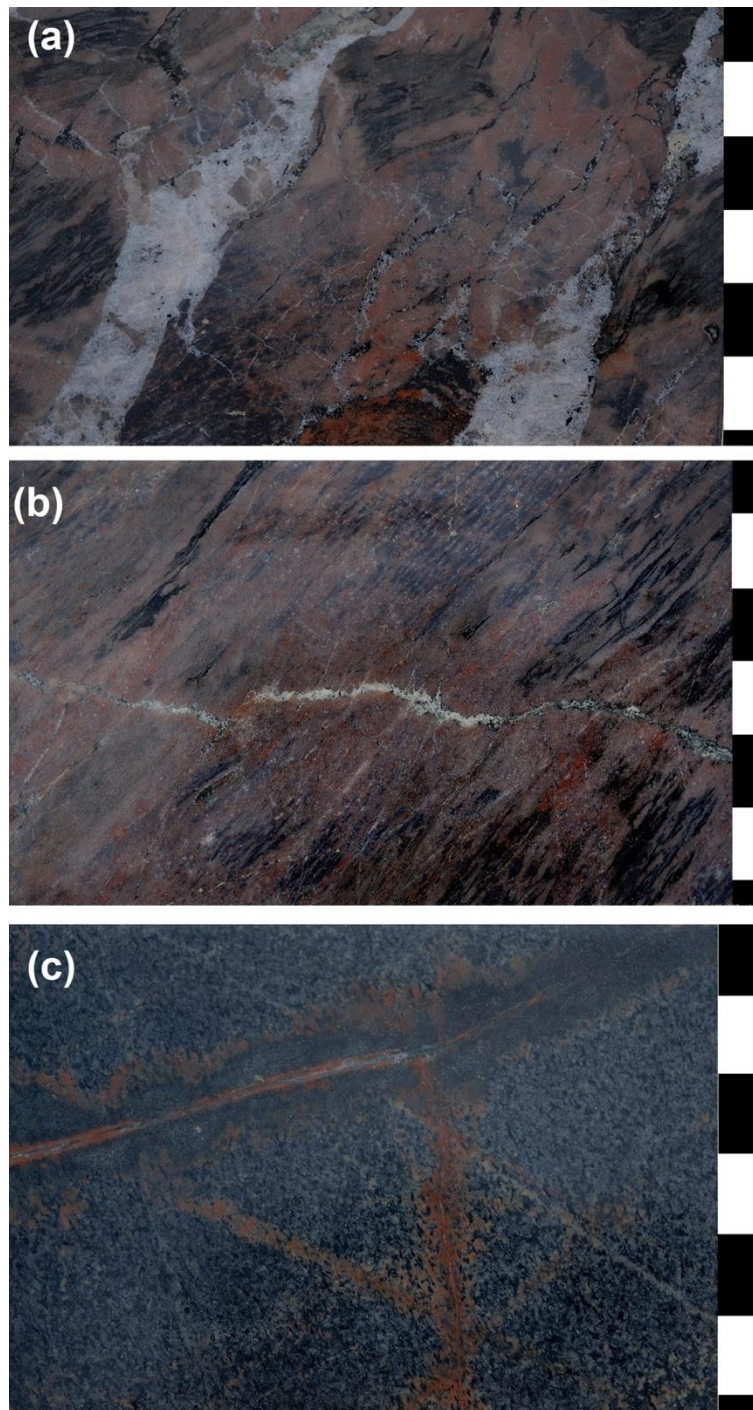


Figure 9: Fenitised lithologies. (a) Crackle brecciated Mount Norna quartzite in core from ES19-DD003 at 42.7 m cut by carbonate veins. Extensive development of secondary K-feldspar fenite that obliterates fabrics in the quartzite. (b) Fenitised quartzite in core from ES19-DD003 at depth interval 42.5 m. Extensive development of secondary K-feldspar fenite that obliterates fabrics in the quartzite. (c) Unit of meta basalt in ES19-DD003 at depth of 34.8 m Extensive development of secondary K-feldspar fenite that obliterates fabrics in the metabasalt.

3.2.3 Magnetite Rich Lithologies

Both ES19-DD001 and ES19-DD003 cores contain abundant and widely distributed magnetite, commonly associated with zones of potassic fenite. Examples are given in Figures 7b & 8b. Presence of magnetite is significant as this is an important mineral phase in IOCG systems.

3.2.4 Sulphide-rich Units of Tuffisite

Distinctive units of carbonate and sulphide-rich tuffisite, a matrix-supported, heterolithic, hydrothermal breccia are observed at ~80-90 m in ES19-DD001 and at ~160 m in ES19-DD003, where they are associated with chalcopyrite-bearing crackle breccias. Typical examples are shown in Figure 9.

The units of tuffisite are interpreted to represent a syn-epithermal mineralisation degassing vent, where volatiles were derived from a deeper igneous source.

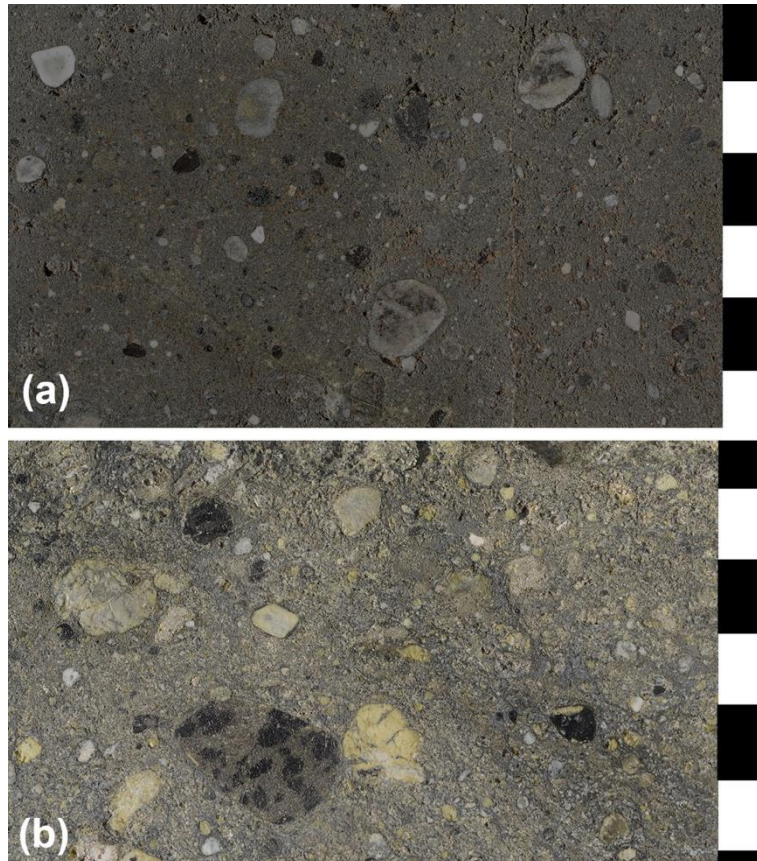


Figure 10: (a) Heterolithic tuffisitic in core from ES19-DD001 at 83.6-84 m (b) Unit of heterolithic tuffisite in core from ES19-DD001 at depth interval 88 - 88.3 m. Matrix appears to be sulphide rich. This lithology was also observed near the bottom of ES19-DD003 at ~160 m associated with crackle breccia. The tuffisite is interpreted as a syn-epithermal mineralisation degassing vent from a deeper igneous intrusion.

3.2.5 Epithermal Veins Cutting Tuffisite

Epithermal textures, such as colloform veins containing crystalline quartz vughs occur in both cores. In ES19-DD001, these veins cut the tuffisite (Figure 10b). This suggests a genetic relationship with the epithermal mineralisation reported previously from the area (Collerson 2019).

The presence of these high-crustal level epithermal lithologies provides a ready explanation for the wide spread Au mineralisation in Ausmex's Mount Freda and Golden Mile prospects.

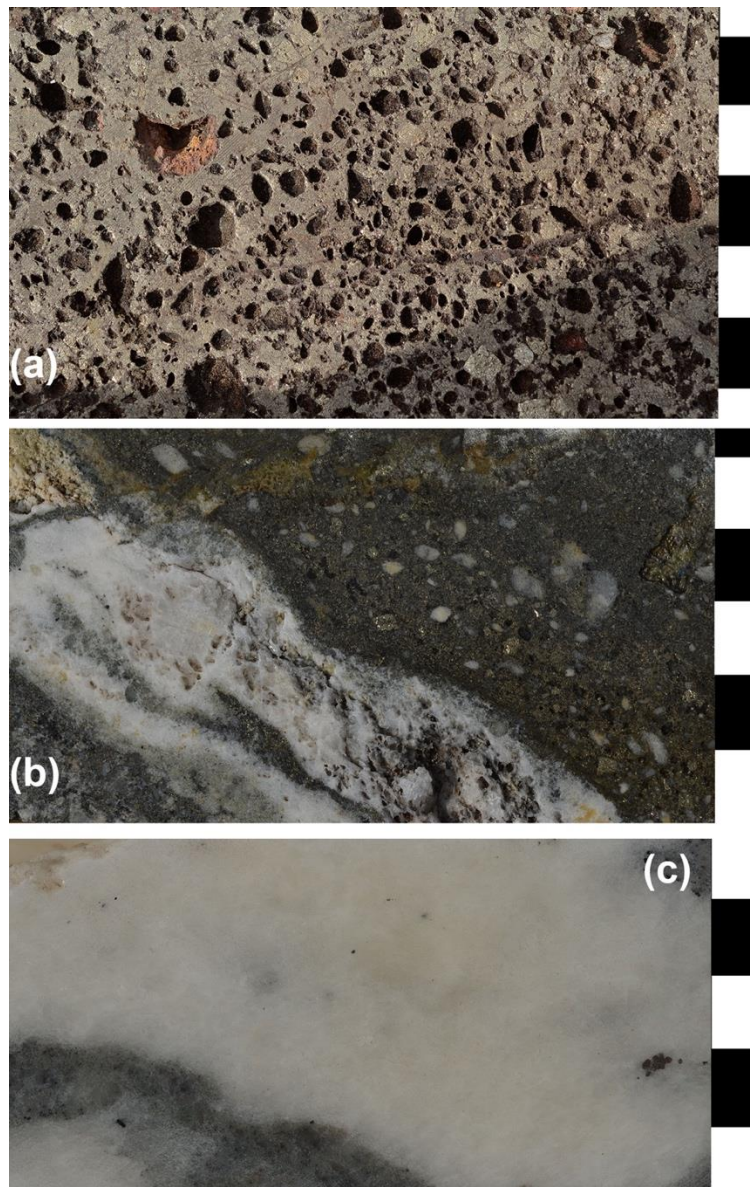


Figure 11: (a) Native Cu and gossanous sulphide unit in core from ES19-DD001 at 59.7 - 59.85 m immediately above sulphide rich tuffisitic unit (b) Epithermal siliceous vugh cutting sulphide-bearing heterolithic tuffisite in core from ES19-DD001 at depth interval 76.5-76.6 m (c) Unit of compositionally variable carbonate in ES19-DD001 at depth of 71.82 - 72 m. This is interpreted as a carbothermal vein associated with the tuffisite - epithermal system.

3.2.6 Gossan and Native Cu

In ES19-DD001, the tuffisite conduit occurs below a unit of native copper and sulphide bearing gossan (Figure 10a). This could indicate that a genetic relationship exists between the tuffisite conduits and possible mineralisation in the vicinity of the magnetic target. Thus, the occurrence of tuffisite and the epithermal textures could be useful vectors for deeper mineralisation.

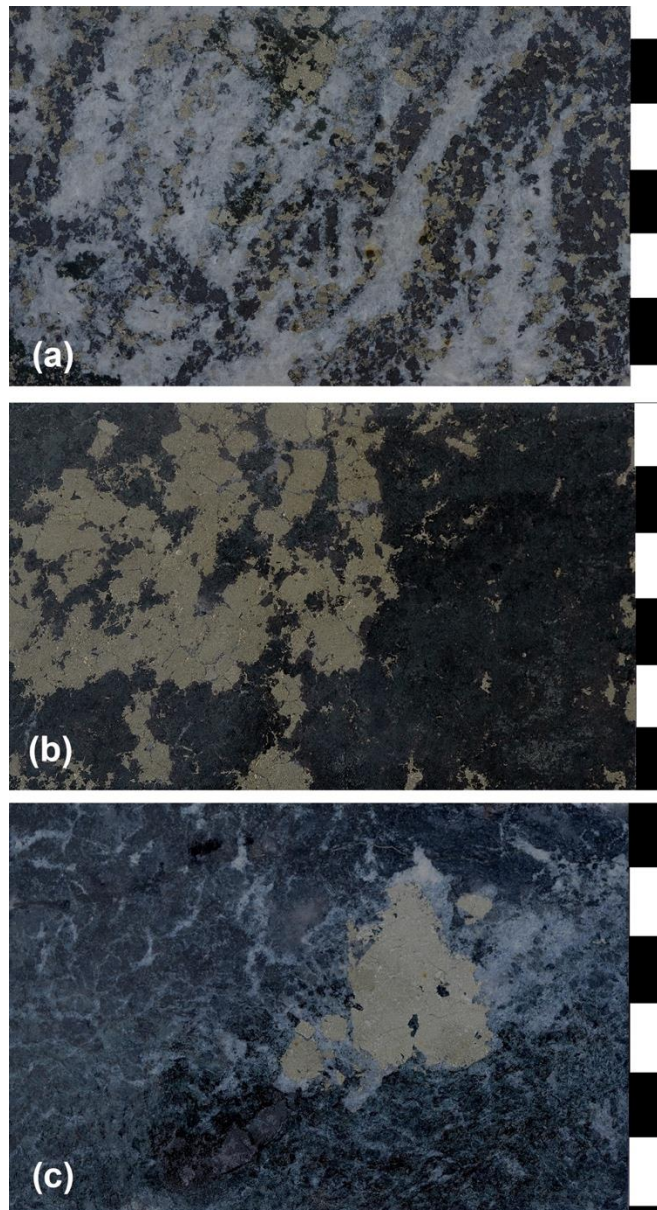


Figure 12: (a) Carbonate-magnetite-sulphide unit in core from ES19-DD003 at 55 - 55.2 m (b) Coarse grained unit of sulphide-bearing pyroxenite in core from ES19-DD003 at depth interval 110.15-110.45 m (c) Unit of sulphide-bearing pyroxene gabbro in ES19-DD003 at depth of 32.1-32.45 m.

3.2.7 Carbo-thermal Carbonate Veins

Carbonate-rich veins of probable carbothermal derivation (see, Mitchell 2005 and Rosatelli et al., (2010) occur throughout both cores (Figure 10c and Figure 12a).

3.2.8 Carbonate-rich Mela-gabbros

Both cores exhibit pyroxene-rich gabbroic units (mela-gabbros) that are locally carbonate-rich with dispersed aggregates of sulphide, including chalcopyrite (Figures 12 b & c).

These gabbroic units, like the pyroxenites, are interpreted to be genetically related. They are both clearly post tectonic, i.e. they were emplaced after thermos-tectonism (deformation) associated with the Isan Orogeny.

3.2.9 Alkali Syenite Dykes

A coarse-grained dyke of alkali pyroxene (?) bearing syenite, that cuts a K-fenitised meta-mafic unit, occurs in ES19-DD003 at 112 - 112.4 m. This dyke is interpreted as a possible late stage differentiate derived from a deeper intrusive source.

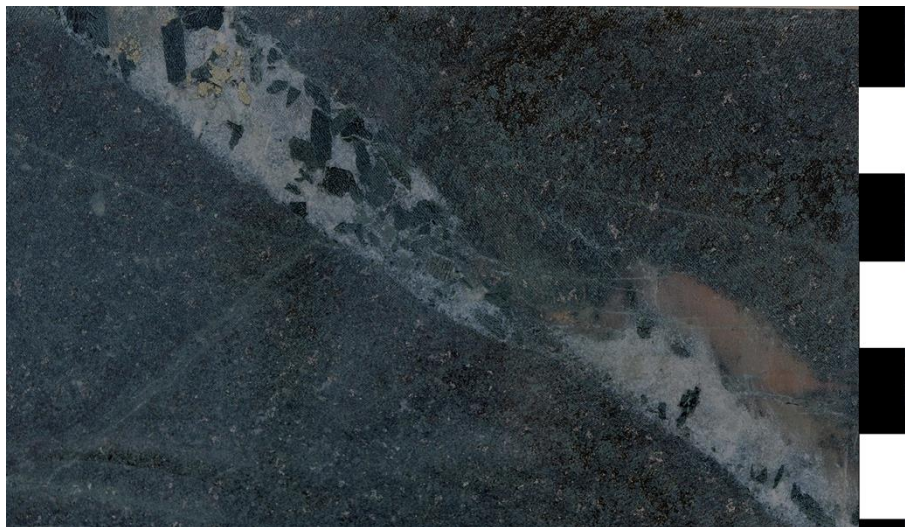


Figure 13: Coarse grained alkali pyroxene (?) bearing syenite (dyke) cutting K-fenitised meta-mafic unit in core from ES19-DD003 at 112 - 112.4 m.

4. ES19-DD001 and ES19-DD003 Assays

4.1 The Tuffisite Breccia System

4.1.1 Chemical Comparison

Assays from DD001 and DD003, summarised in Table 2, confirm the metallogenic significance of the tuffisite breccia system as the plumbing system that enabled the transport of metal responsible for IOCG or possible porphyry mineralisation in the Cloncurry district.

Tuffisite breccias in DD001 and DD003 cores have high metal contents, e.g., copper (1060 to 9640 ppm; average 8420 ± 3321 and 3290 to 21,700 (2.17%) to ppm; average 8530 ± 7612) gold (0.03 to 0.69 g/t; average 0.36 ± 0.18 g/t and 0.19 to 3.36 g/t; average 1.29 ± 1.79 g/t), nickel (107 to 599 ppm; average 339 ± 121 ppm and 92 to 309 ppm; average 233 ± 105 ppm), cobalt (124.5 to 496 ppm; average 295 ± 98 ppm and 82.6 to 222 ppm; average 192 ± 70 ppm) and molybdenum (3.29 to 12.7 ppm; average 6.63 ± 3.37 ppm and 3.84 to 11.1 ppm; average 5.26 ± 1.36 ppm). The tuffisite also contains anomalous bismuth, sulphur and tellurium e.g., bismuth (0.07 to 2.52 ppm; average 0.80 ± 0.89 and 0.28 to 1.24 ppm; average 0.64 ± 0.52 ppm), sulphur (2.8 to 10 wt.%; average 8.2 ± 2.2 and 3.25 to 6.43 wt. %; average 5.6 ± 1.4 wt. %) and tellurium (3.29 to 12.7 ppm; average 6.63 ± 3.37 and 0.7 to 3 ppm; average 0.64 ± 0.52 ppm).

The native Cu and gossanous unit in DD001 exhibits similar or even more extreme levels of enrichment, e.g., copper (1.03 to 4.32 wt. %; average 2.65 ± 1.37 wt. %) gold (0.33 to 2.07g/t; average 1.08 ± 0.64 g/t), nickel (443 to 1100 ppm; average 723 ± 251 ppm), cobalt (177 to 881 ppm; average 508 ± 314 ppm) and molybdenum (8.75 to 70.4 ppm; average 32 ± 23.8 ppm). This unit also contains anomalous bismuth, sulphur and tellurium e.g., bismuth (0.43 to 1.73 ppm; average 0.93 ± 0.51 ppm), sulphur (5.7 to 10 wt.%; average 9.1 ± 1.9 wt.%) and tellurium (3.42 to 7.46 ppm; average 5.1 ± 1.7 ppm).

When compared to the mean composition of 155 assays of Soldiers Cap Group host rocks in DD001, the tuffisite and gossanous unit are clearly anomalous. For example, copper (553 ± 1075 ppm), gold (0.02 to 0.06 g/t), nickel (90 ± 114 ppm), cobalt (102 ± 135 ppm), molybdenum (2.26 ± 3.14 ppm), bismuth (0.11 ± 0.22 ppm), sulphur (1.14 ± 2.33 wt.%) and tellurium (0.29 ± 0.62 ppm).

Although earlier studies of IOCG systems in the Cloncurry district have interpreted the Cu, Au, REE, actinides, S and volatiles to have been sourced from the igneous rocks (granitoids) associated with the Williams-Naraku Batholith via magmatic-hydrothermal fluids (Williams et al., 2015), given the element association reported in the current and

previous studies (e.g. Collerson, 2019), a more plausible explanation is that the metals were derived from an ultramafic to mafic alkaline source.

Table 2: Chemical Variations in Tuffisite and Gossan

	From Depth (m)	To Depth (m)	Au (ppm)	Ag (ppm)	Sc (ppm)	Co (ppm)	Cu (ppm)	Ni (ppm)	Mo (ppm)	Zr (ppm)	Y (ppm)	W (ppm)	Te (ppm)	Bi (ppm)	Sb (ppm)	S wt. %
ES19-DD001																
Gossan	59.5	60	2.07	1.21	22.1	881	20100	1100	8.75	6.7	20.3	5.1	7.46	1.73	0.12	10.0
	60	60.5	1.11	0.82	28.3	804	20900	814	16.3	27.3	19	3.5	5.81	1.03	0.14	10.0
	60.5	62	1.11	1.51	55	176.5	38200	572	33.7	54.1	47.2	5.2	5.29	0.43	0.12	5.7
	62	62.5	0.79	1.41	11.3	333	43200	443	70.4	101	39.7	21.8	3.53	0.53	0.18	10.0
	62.5	63	0.33	0.48	9.9	347	10300	688	31	79	21	14	3.42	0.95	0.12	10.0
Average			1.08	1.09	25.3	508	26540	723	32.0	53.6	29.4	9.9	5.1	0.93	0.14	9.1
SD			0.64	0.43	18.3	314	13698	251	23.8	38.0	13.1	7.8	1.7	0.51	0.03	1.9
Tuffisite																
	80	81	0.46	1.52	31.1	315	5360	333	3.29	65	37.1	8.9	3.29	0.22	0.24	7.8
	81	81.5	0.36	0.54	29.5	438	6400	333	3.82	67.4	30.5	2.2	3.82	0.19	0.35	8.1
	81.5	82	0.3	0.97	28.8	496	6750	449	4.14	52.6	36.1	3.2	4.14	0.28	0.29	10.0
	82	83	0.12	0.56	36	145	4490	136	3.73	96.1	38.8	2.9	3.73	0.09	0.16	3.9
	83	83.5	0.03	0.3	34.7	124.5	2030	107	4.32	113	36.1	3.7	4.32	0.07	0.23	2.8
	83.5	84	0.41	0.74	27.7	261	9640	331	6	45.5	31.1	2.1	6	0.28	0.16	8.0
	84	84.5	0.5	0.8	25.4	238	11550	326	6.89	40.5	34.3	2.3	6.89	0.28	0.22	7.8
	84.5	85	0.42	0.83	26	255	11500	282	5.47	39.6	33.2	2.3	5.47	0.26	0.28	7.4
	85	85.5	0.43	0.95	27.7	321	11100	384	4.7	30.3	41.1	2.3	4.7	0.47	0.41	9.7
	85.5	86	0.48	0.81	25.9	304	10600	320	4.31	28	42.6	2	4.31	0.48	0.31	9.1
	86	86.5	0.11	0.4	26.9	221	5230	335	5.78	40.6	30.8	2.1	5.78	0.87	0.4	8.0
	86.5	87	0.36	0.56	29.3	355	8220	319	10.5	65.6	24.1	2.4	10.5	1.32	0.68	10.0
	87	87.5	0.49	0.94	24.8	285	12600	599	12.65	60	25.7	3.1	12.65	2.25	0.22	10.0
	87.5	88	0.69	0.87	25.3	366	8930	497	11.15	54.5	27.8	2.5	11.15	2.43	0.47	10.0
	88	88.5	0.18	0.88	26.4	304	11900	334	12.7	59.7	29.2	2.7	12.7	2.52	0.53	10.0
Average			0.36	0.78	28.37	295	8420	339	6.63	57.2	33.2	2.98	6.63	0.80	0.33	8.2
SD			0.18	0.29	3.36	98	3221	121	3.37	23.1	5.5	1.71	3.37	0.89	0.15	2.2
Core BG																
Average	n=151		0.02	0.18	37.46	102	553	90	2.26	66.6	32.3	4.70	0.29	0.11	0.26	1.14
SD			0.06	1.04	7.82	135	1075	114	3.14	48.1	20.9	8.86	0.62	0.22	0.16	2.33
ES19-DD003																
Tuffisite	159.52	160	0.22	0.18	30.9	87.5	3470	98.7	11.1	89.6	21.9	20.4	0.9	0.53	0.05	3.63
	160	160.38	0.26	0.18	25.2	82.6	3290	92	8.94	78.8	17.1	25	0.7	0.38	0.11	3.25
	160.38	161.35	3.36	1.2	17.9	111.5	21700	112.5	6.56	84.5	13.6	57.5	3	1.24	0.13	3.96
	161.35	162	0.19	0.33	20.9	241	6350	309	5.38	47.9	18.3	8.6	1.37	0.28	0.07	6.28
	162	163	0.32	0.48	23.8	222	7840	276	3.84	40.5	33.6	2.8	1.73	0.4	0.27	6.43
Average			1.29	0.67	20.87	192	11963	233	5.26	57.6	21.8	23.0	2.03	0.64	0.16	5.6
SD			1.79	0.47	2.95	70	8465	105	1.36	23.6	10.5	30.0	0.86	0.52	0.10	1.4

4.1.2 Transition Elements

Covariation between the transition elements, nickel, cobalt and copper in the tuffisite from ES19DD001 and ES19DD003, and in the native Cu-gossanous interval in ES19DD001 are shown in Figure 14 a and b. The tuffisite unit in both cores have similar concentrations of Cu, Co and Ni are either strongly (Co-Ni) or weakly (Cu-Ni) positively correlated. Samples with the highest Cu values are interpreted to reflect supergene enrichment.

The gossanous samples from ES19DD00 lie on the same Co-Ni correlation vector indicating that they have similar Co/Ni ratios to the metal-rich tuffisites. This confirms their genetic relationship.

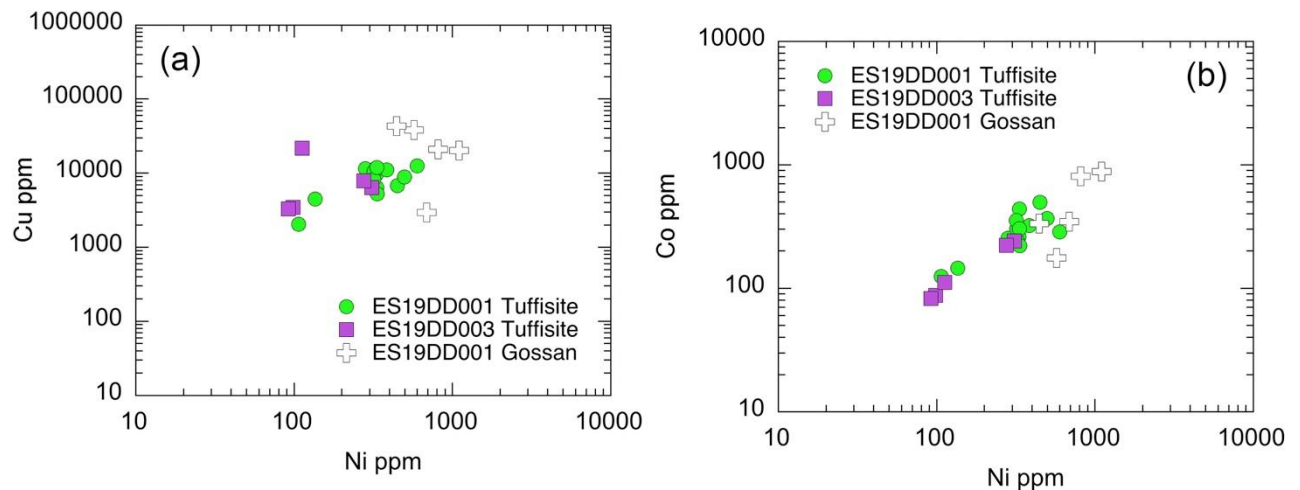


Figure 14: Covariation between Cu and Ni (a) and Co and Ni (b) in tuffisite from ES19DD001 and ES19DD003, and in the native Cu-gossanous interval.

4.1.3 Scandium

The tuffisite and gossan are enriched in Sc relative to the upper continental crust Figure 15. Upper continental crust has an average of 12 ppm Sc (Taylor and McLelland, 1985).

Tuffisite in both cores have similar Sc and Ni contents. These define two populations that are interpreted to reflect variable amounts of sulphide in the samples that were analysed. Sc in the gossan ranges from ~10 to 60 ppm. This enrichment may reflect supergene processes.

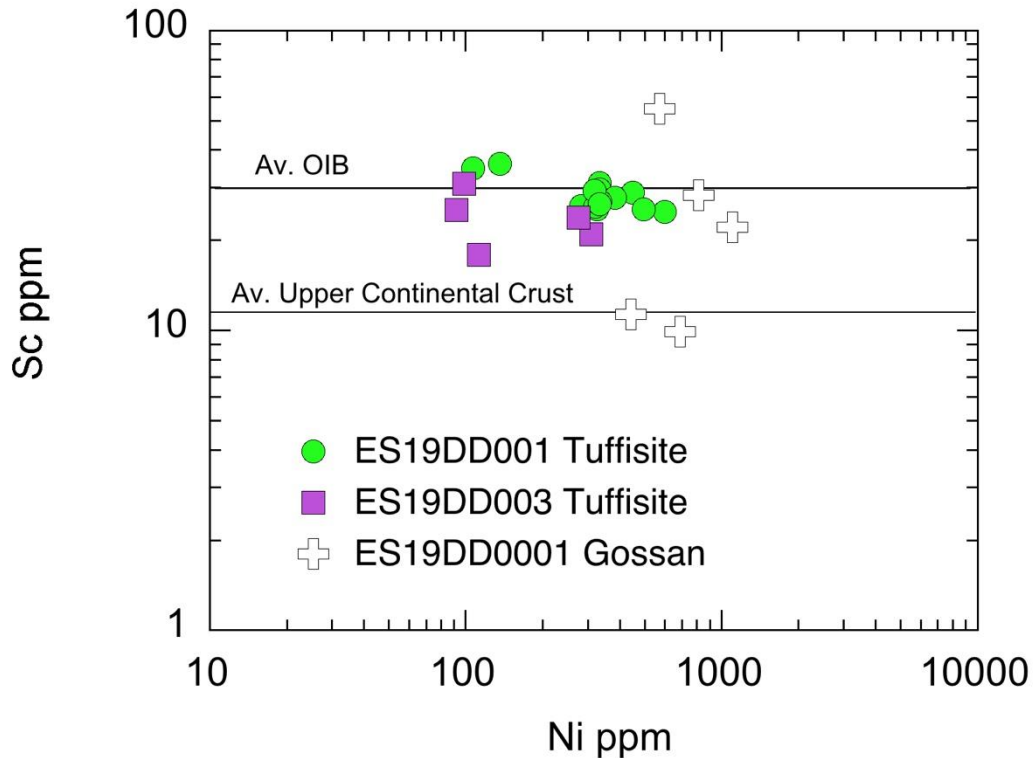


Figure 15: Variation in Sc and Ni in tuffisite and gossan from ES19DD001 and ES19DD003

4.1.4 Rare Earth Systematics

In terrestrial rocks and meteorites, the REEs with even-atomic numbers are more abundant than the adjacent REE odd-atomic numbered REE. This reflects the Oddo-Harkins Rule and is caused by differences in binding energies and thus relative stabilities of nuclei with paired and unpaired nucleons. To overcome this pattern, REE abundances are normalised to the measured REE abundances in chondritic meteorites, such as C1 chondrites - the composition of the solar nebular (Anders and Grevesse, 1989). The normalised REE data are then arranged in order of increasing atomic numbers from La to Lu and plotted on a logarithmic scale.

Chondrite normalised REE data for the tuffisites from ES19DD001 and ES19DD003 are plotted in Figures 16a and 16c. The patterns for the tuffisites from both cores are concave down with La_N ranging from 332 to 882 and Lu_N from 31.5 to 86 in (a) and La_N ranging from 291 to 643 and Lu_N from 13 to 49.5 in (b). There is a slight -ive Eu anomaly in (a) and a more distinct anomaly in (b).

The most remarkable feature seen in Figure 16a, is the homogeneity of the pattern for ES19DD001 over 8.5 m of core interval. Given the lithological heterogeneity of the host rocks, these homogeneous fractionation patterns could indicate a high fluid/rock ratio in the tuffisite pipe which enabled efficient mixing. This effect would be expected in a hydrothermal vent.

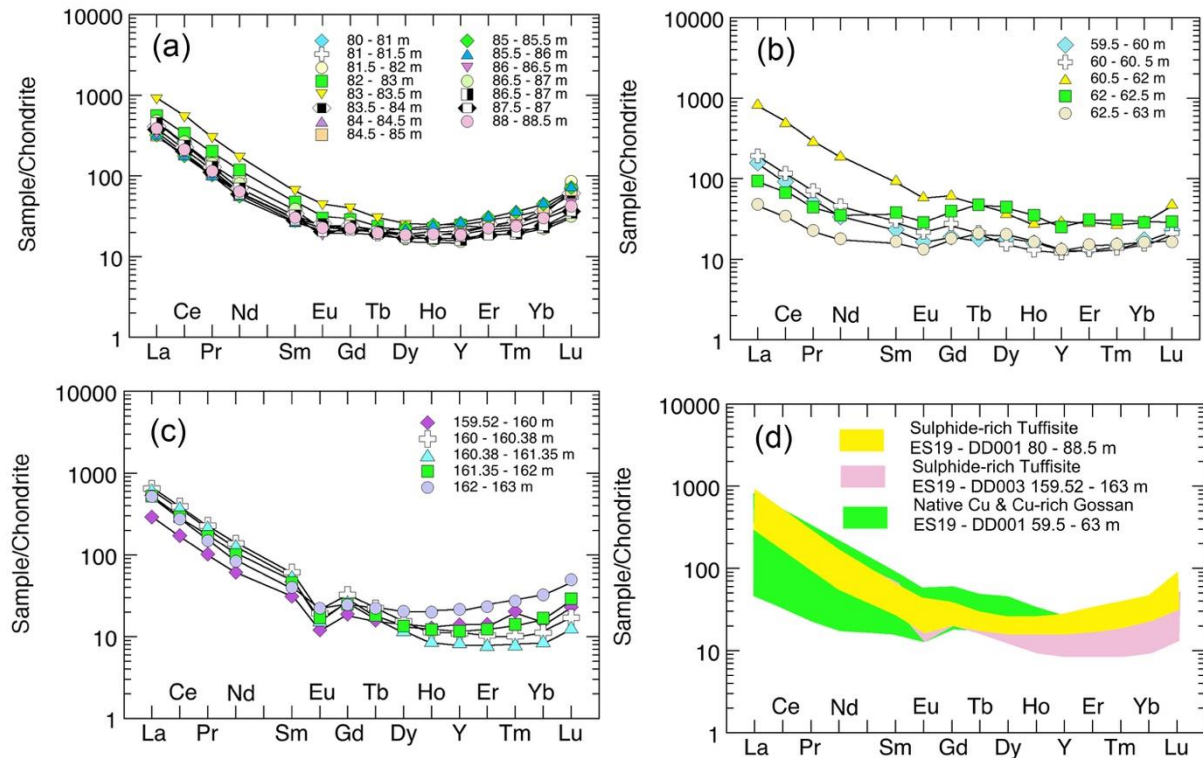


Figure 16; Chondrite normalized REE plots showing patterns for tuffisites from (a) ES19DD001, (b) ES19DD003 and the native Cu gossan interval in ES19DD001. The patterns are compared in (d). Using normalizing data from McDonough and Sun (1995).

4.1.5 La/Yb versus Total Rare Earth Discrimination Projection

La/Yb (a proxy for LREE/HREE ratio) plotted against total REE concentrations is a very useful diagram to discriminate between REE sources (Loubert *et al.*, 1972).

The tuffisite samples from both cores display similar compositions (Figure 17), which suggests that they are genetically related from a common REE source. This confirms the lithological correlation that has been made both between cores. Importantly, the samples plot on a vector that extends from fractionated alkaline intrusions to carbonatites.

As the native Cu - gossan interval lies along the same vector, this strongly suggests that Cu, Au and other metals, including Ni and Co were derived from the same source alkaline igneous source.

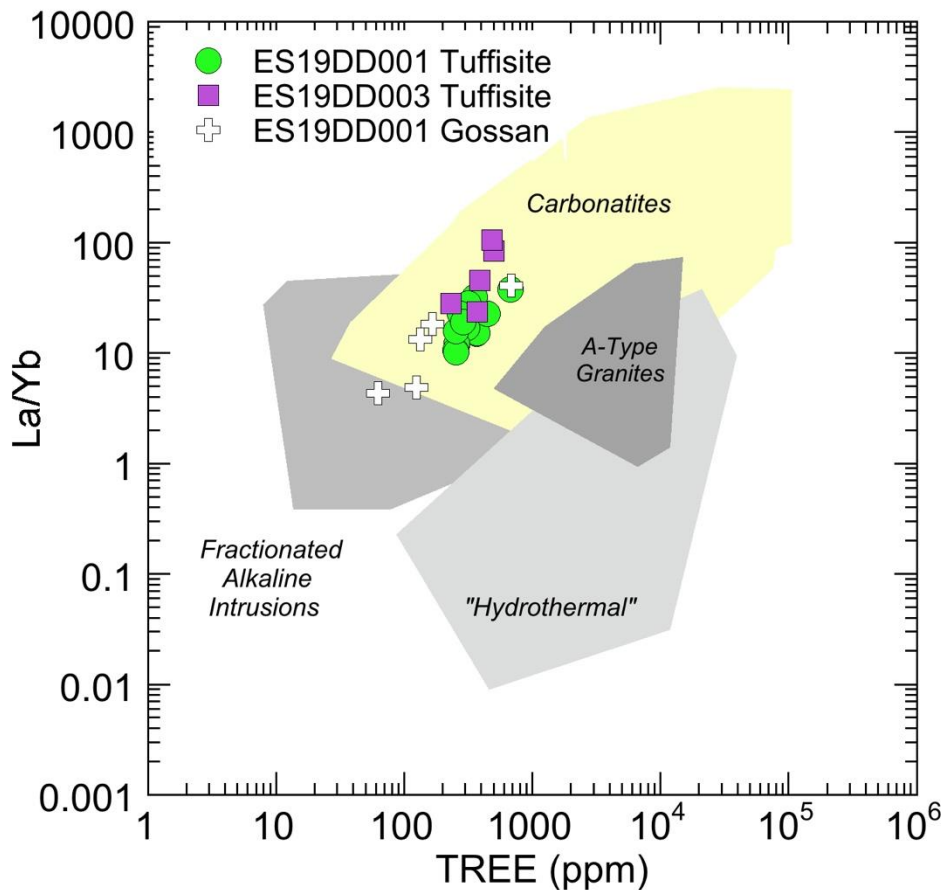


Figure 17: La/Yb vs TREES showing that the tuffisite from both cores and the gossan are related by fractionation.

4.1.6 CHARAC Ratio Systematics

Ratios of the high field strength elements Zr and Hf, as well as Y and the heavy rare earth element Ho, are useful to evaluate the nature of hydrothermal processes in mineral systems. These so called CHARAC ratios (Y/Ho and Zr/Hf) enable magmatic source characteristics in mineral deposits to be distinguished from systems affected by hydrothermal processes (Bau, 1996).

If a geochemical system is characterized by CHARGE and-RADIUS-CONTROLLED (CHARAC) trace element behaviour, elements with similar charge and ionic radius, such as the twin pairs Y-Ho and Zr-Hf, should display coherent behaviour during crystallization and retain their respective chondritic ratios. Mantle-derived igneous rocks, for example, have Y/Ho and Zr/Hf ratios close to the ratios recorded by chondritic meteorites, viz. 28 and 38.

Carbonatites and alkaline igneous systems display this characteristic (de Andrade et al., 2002). These ratios are within error of values exhibited by mantle plume

generated ocean island basalts (OIBs) viz., $Y/Ho = 27.7 \pm 2.7$ and $Zr/Hf = 36.6 \pm 2.9$ (Bau, 1996). Thus, they are useful indicators of mantle plume magmatism.

However, Y can be fractionated from Ho in medium-temperature F-rich aqueous fluids in hydrothermal systems due to fluoride complexation (Bau and Dulski, 1995; Buhn, 2008). Similar fractionation also occurs in F-rich peralkaline granitic melts (Bau and Dulski, 1995; Buhn, 2008).

The tuffisites from ES19DD001 and ES19DD003 fall within the CHARAC field with generally chondritic Y/Ho and Zr/Hf ratios (Figure 18). However, Y/Ho ratios of the native Cu - gossanous samples range from chondritic to sub-chondritic. This indicates fractionation of Y from Ho by fluoride complexation.

Importantly, F is an important component in IOCG systems and plays a role in hydrothermal metal transport. Such halogen-rich fluid compositions are conducive to fluid - metal transport (Liu et al., 2011; Landis and Hofstra, 2012; Brugger et al., 2016) where metals are transported as aqueous complexes. Dissociation of these complexes in response to changes of the hydrothermal environment caused by a variety of processes, e.g., fluid-rock interaction, fluid mixing, cooling, or phase separation, results in the precipitation of minerals (Seward and Barnes, 1997).

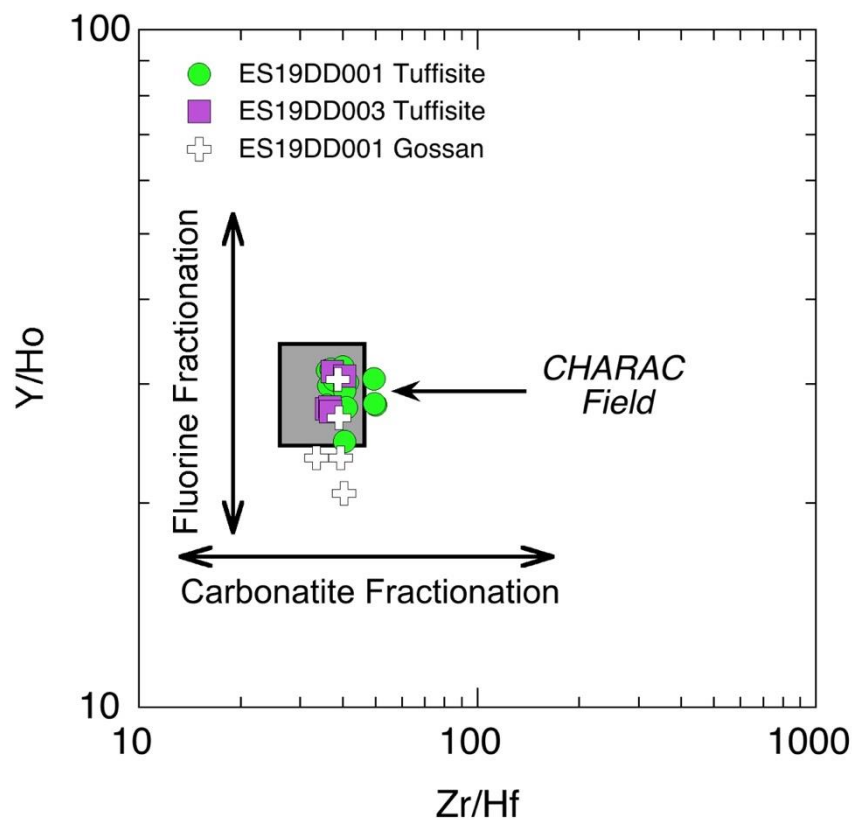


Figure 18: CHARAC plot showing data for the tuffisite and gossan

4.1.8 Constraints from Primitive Mantle Normalised Ta/U and Nb/Th ratios

This projection, from Niu and Batiza (1997) and Niu et al., (1999) shows that plume-derived magmas, formed by melting in lower mantle upwellings (EM1 and HIMU , Table 3), plot close to unity. Whereas, magmas contamination by continental crust, crustal fluids, or fluids derived from subducted slabs Kessel et al., (2005), lie in the lower left-hand quadrant, with Ta/U_{PMN} of ~0.01 and Nb/Th_{PMN} of ~0.1.

Table 3: Nb, Ta, U and Th, Ta/U_N and Nb/Th_N

From	To	Nb ppm	Ta ppm	U ppm	Th ppm	Ta/U(ppm)	Nb/Th (ppm)
ES19DD001	Gossan						
59.5	60	0.5		79.9	1.33		0.045
60	60.5	1.6	0.12	93.6	3.28	0.001	0.059
60.5	62	4.6	0.29	243	10	0.001	0.056
62	62.5	7.5	0.36	755	83.6	0.00003	0.011
62.5	63	4.2	0.24	399	33.1	0.00003	0.015
ES19DD001	Tuffisite						
80	81	8.3	0.31	19.2	2.52	0.009	0.398
81	81.5	5.8	0.28	35.2	2.99	0.004	0.234
81.5	82	4.7	0.21	19	2.3	0.006	0.247
82	83	9.7	0.43	27.1	2.85	0.009	0.411
83	83.5	8.9	0.47	29.7	3.46	0.009	0.311
83.5	84	3.1	0.17	11.6	2.79	0.008	0.134
84	84.5	2.3	0.14	11.5	2.84	0.007	0.098
84.5	85	2.8	0.15	10.5	2.5	0.008	0.135
85	85.5	2.2	0.12	8.2	2.45	0.008	0.108
85.5	86	2	0.11	8.2	2.47	0.007	0.098
86	86.5	2.9	0.16	7.6	3.18	0.012	0.110
86.5	87	4.3	0.26	13.4	5.49	0.011	0.095
87	87.5	3.2	0.19	17.9	5.34	0.006	0.072
87.5	88	3	0.19	15.4	4.38	0.007	0.083
88	88.5	3.3	0.21	15.6	4.83	0.007	0.083
ES19DD003	Tuffisite						
159.52	160	4.7	0.26	19.9	4.8	0.007	0.118
160	160.38	3.3	0.19	14.9	4.15	0.007	0.096
160.38	161.35	3.4	0.17	13	5.02	0.007	0.082
161.35	162	2.6	0.16	11.3	3.82	0.008	0.082
162	163	3.4	0.17	11.6	3.96	0.008	0.104
Plume End-members							
EM1		97.6	6.1	2.9	11.4	1.242	1.052
HIMU		104.8	6.1	2.2	8.1	1.514	1.564

The tuffisite from ES19DD001 and ES19DD003 virtually the same Ta/U_{PMN} ratios ~0.01 but they show a spread in Nb/Th_{PMN} (Figure 19a). The data are interpreted to contamination of the plume component (which contributed Au, Ni and Co) and by slab derived fluids (which contributed Cu). This vector differs from the Ta/U_{PMN} and Nb/Th_{PMN} field of the Soldiers Cap Belt country rocks (Figure 19b), indicating that this

was unlikely to be the source of metals. Separation of the sulphide rich gossan and supergene processes increased U and Th resulting in even lower Ta/U_{PMN} and Nb/Th_{PMN} . There is a strong possibility that the pyroxenite dykes identified in the core could represent this post-Soldiers Cap plume component.

In view of the high concentrations of transition group metals in the tuffisite and native Cu-gossan, the low Ta/U_{PMN} and Nb/Th_{PMN} component is unlikely to be the result of crustal contamination. A more plausible explanation is that it could reflect the presence of a component, from which a Nb-Ta mineral phase has been fractionated.

Discovery of this component represents a future exploration challenge in the district. It is most likely associated with an elusive carbonatite, the presence of which has been shown by the REE element systematics.

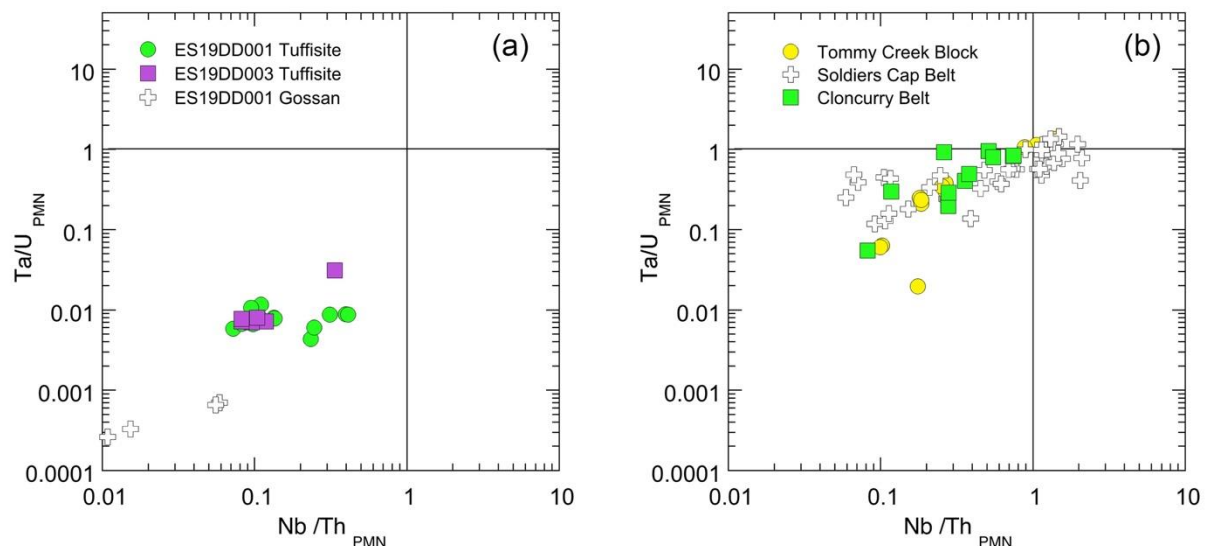


Figure 19: Primitive mantle normalised Ta/U and Nb/Th ratios, calculated from data in Table using primitive mantle values from McDonough and Sun (1995) and Lyubetskaya and Korenaga (2007). (a) Shows consistent data from the tuffisite and (b) shows normalised Ta/U and Nb/Th ratios for mafic lithologies from the Soldiers Cap Belt which are cut by the tuffisite.

4.1.9 Gold Tellurium and Bismuth

Tellurium and bismuth are commonly associated with gold in epithermal systems (e.g. Tooth et al., 2008). Figure 18 shows data for the tuffisite and the gossan. Au is broadly positively correlated with Te (Figure 18a). Bi and Au are well correlated in tuffisite from both cores. This indicates the possible formation of Au-Bi tellurides in the epithermal system.

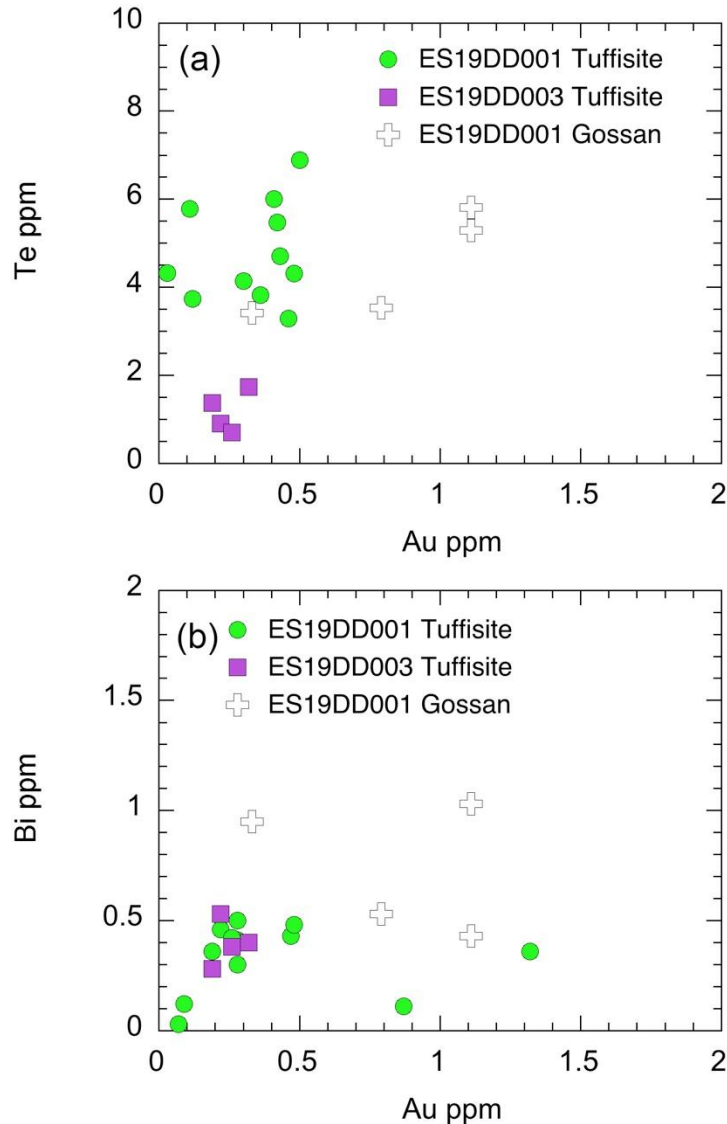


Figure 20: Covariation between (a) Te and Au, and (b) Bi and Au in the tuffisite and gossan

4.1.10 Molar Cu/Au Systematics and Metal Sources

Background

Cu/Au ratios and bulk metal content, specifically Au grade, in porphyry-style Cu–Au ± Mo deposits are controlled in part by the chemistry of the magmatic fluid source (Sillitoe 1997; Heinrich et al. 2005). The wide range of Cu and Au grades in deposits (Kesler 1973; Singer et al. 2005) is also affected by at least two additional factors. First, fluid phase separation into brine and vapour, causes selective Cu–Au fractionation into the vapour (Heinrich et al. 1999). Second, ore grades are controlled by the precipitation efficiency of Cu–sulphides and native gold during fluid cooling (e.g., Ulrich et al. 2001). Thirdly there is the possibility of selective Au enrichment in primary auriferous Cu–sulphides e.g., in bornite (Kesler et al. 2002). **Finally, the Au grade of porphyry-style mineral systems increases with decreasing depth of ore deposition and hence lithostatic pressure (e.g., Sillitoe 1997), showing significant enrichment in associated epithermal systems.**

Relationships between Au grade and tectonic setting, magnetite content in potassic alteration zones, deposit morphology, and associated rock types indicate that porphyry-style ore deposits and IOCG deposits range between two end-member types (Kesler 1973; Sinclair et al. 1982; Sillitoe 1979). **The most Au-rich Cu–Au deposits, which are commonly associated with mafic intrusive rocks are emplaced at around 1 km and usually contain abundant magnetite in the potassic alteration zone. The presence of epithermal mineralisation at Mt Freda indicates that it lies within this 1,000 m window.**

The Cu/Au ratio of porphyry-style and IOCG ore deposits is likely to be controlled by magma source Sillitoe (1997) and also with the physical - chemical evolution of the ore-forming hydrothermal fluids.

Magma source plays an important role in formation of large Au - rich porphyry-style deposits containing over 200 t of Au in the circum-Pacific region, where formation of these Tier One Au-rich magmatic-hydrothermal ore deposits are interpreted to result from oxidized magmatism which is induced by post-subduction partial melting of stalled oceanic lithospheric slabs, or by mantle wedge melting.

In both cases, the heat for melting and precious metal flux (indicated by presence of Pt and Pd in many of these deposits) is contributed by upwelling mantle plumes that pass through slab tears (Collerson et al., 2015). The former process produces Au-rich adakites while the latter, favors the development of high-K calc-alkaline to shoshonitic compositions which host epithermal Au and porphyry.

A positive correlation between Cu/Au ratio and depth (Sillitoe 1997), suggests that magma source is not the sole factor determining the bulk metal ratio. According to Murakami et al., (2010), the systematic variation of Au/Cu ratios of porphyry-style ore deposits with depth and pressure of ore formation is related to the change in density of cooling magmatic hydrothermal fluids. Fluid pressure controls the extent of fluid phase separation into brine and vapor, resulting in fractionation of ore-forming components. Fluid density and temperature also affects the differential solubility and selective precipitation of ore minerals. This is reflected in the Au enrichment seen in epithermal vein deposits at shallow crustal levels.

The presence of comagmatic extrusive and sub-volcanic activity in gold-mineralized igneous centers indicates relatively shallow depth of ore deposition (Sillitoe 1997). Giant Au and Te - epithermal deposits are commonly associated with alkalic magmas (e.g., Cripple Creek - Thompson et al., 1985; Porgera: Richards 1992).

Molar Cu/Au ratios in representative alkaline and calc alkaline Au and Cu-Au mineral systems are shown in Table 4. Alkaline systems generally exhibit molar Cu/Au ratios that are lower than molar Cu/Au ratios in deposits hosted by calc alkaline lithologies. Galor Creek in British Columbia an epithermal dominated porphyry deposit has the low molar Cu/Au ratio typical of epithermal deposits.

Table 4: Cu-Au Systematics of Au-rich deposits

		Cu wt.	Cu ppm	Cu moles	Au g/t	Au moles	Cu/Au molar	Magma
Kalmakyr	Uzbekistan	2.39	23863	375.49	4.09	0.0208	21971	A ¹
Kalmakyr	Uzbekistan	0.04	433	6.82	0.05	0.0003	26648	A
Grasberg	Irian Jaya	1.13	11300	177.81	1.05	0.0053	33356	A
Bingham	Utah	0.88	8800	138.47	0.5	0.0025	54550	A-SHO ²
Bingham	Utah	1.60	16031	252.26	4.14	0.0210	13707	A
Pebble	Alaska	0.3	3000	47.21	0.34	0.0017	27348	A
Kalmakyr	Uzbekistan	0.4	4000	62.94	0.51	0.0026	24309	A
Dal'neye	Uzbekistan	0.59	5900	92.84	0.69	0.0035	26503	A
Galor	BC Canada	17	170000	2675.06	64.00	0.3249	8233	A
Cadia	NSW	0.31	3100	48.78	0.77	0.0039	12478	A-SHO
Goonumbla	NSW	0.5	5000	78.68	0.5	0.0025	30994	A-SHO
Panguna	Bougainville	0.46	4600	72.38	0.57	0.0029	25013	A
Peschanka	Kamchatka	0.51	5100	80.25	0.42	0.0021	37636	A-SHO
Mamut	Malaysia	20	200000	3147.13	15.20	0.0772	40782	A
Mt Milligan	BC Canada	6.8	68000	1070.02	18.50	0.0939	11392	A
Mt Polley	BC Canada	21	210000	3304.48	23.60	0.1198	27579	A
Afton	BC Canada	1.5	15000	236.03	1.20	0.0061	38742	A
Ajax	BC Canada	0.3	3000	47.21	0.19	0.0010	48939	A
Bajo de la	Argentina	0.52	5200	81.83	0.67	0.0034	24055	K-CA ³
Batu Hijau	Indonesia	0.44	4400	69.24	0.35	0.0018	38965	CA
Ok Tedi	PNG	0.64	6400	100.71	0.64	0.0032	30994	A
Frieda	PNG	0.61	6100	95.99	0.32	0.0016	59083	K-CA
Oyu Tolgoi	Mongolia	0.83	8300	130.61	0.32	0.0016	80392	CA
Sar	Iran	1.2	12000	188.83	0.27	0.0014	137753	CA
La	Chile	1.15	11500	180.96	0.19	0.0010	187598	CA
El Teniente	Chile	0.63	6300	99.13	0.035	0.0002	557901	CA
Olympic	Australia	1.2	12000	188.84	0.5	0.00253	74387	Alkaline (?)
Prominent	Australia	0.98	9800	154.21	0.75	0.00381	40499	Alkaline (?)

¹ A - Alkaline Magma

² A-SHO - Shoshonite Magma

³ K-CA - High K Calc alkaline Magma

⁴ IOCG with alkaline magmatic metal source

The Olympic Dam and Prominent Hill IOCG deposits in South Australia associated with the alkaline Hiltaba Intrusive Suite also have molar Cu/Au ratios

that a similar to the alkaline hosed porphyry systems (Table 4).

Molar Cu/Au ratios for the tuffisites and gossan from ES19DD001 and ES19DD003 are shown in Table 5.

Table 5: Molar Cu/Au Ratios for DD001 and DD003

		Cu ppm	Au g/t	molar Cu/Au
Native Cu and Gossan		20100	2.07	30096
ES19-DD001 59.5-63		20900	1.11	58359
		38200	1.11	106666
		43200	0.79	169489
		10300	0.33	96740
Average				92270
SD				52928
Sulphide-rich Tuffisite		5360	0.46	36115
ES19-DD001 80-88.5		6400	0.36	55101
		6750	0.3	69738
		4490	0.12	115971
		2030	0.03	209729
		9640	0.41	72875
		11550	0.5	71597
		11500	0.42	84866
		11100	0.43	80009
		10600	0.48	68446
		5230	0.11	147365
		8220	0.36	70771
		12600	0.49	79700
		8930	0.69	40113
		11900	0.18	204908
Average				93820
SD				53455
Sulphide-rich Tuffisite		3470	0.22	48887
ES-19-DD003		3290	0.26	39220
159.52-163m		21700	3.36	20017
		6350	0.19	103587
		7840	0.32	75937
Average				52928
SD				35841

For comparison molar Cu/Au ratios for the Eastern Succession IOCGs are shown in Table 6.

Table 6: Cu-Au Systematics of Eastern Succession IOCG Deposits

	Cu %	Cu ppm	moles Cu	Au g/t	Moles Au	Cu/Au (molar ratio)
Porter Geoconsultancy						
Ernest Henry	1.1	11000	173.09	0.54	0.0027	63137
Ernest Henry	1.25	12500	196.70	0.65	0.0033	59605
Osborne	3.51	35100	552.32	1.49	0.0076	73014
Starra	1.8	18000	283.24	3.8	0.0193	14682
Jubilee	3.37	33700	530.29	2.28	0.0116	45812
Kalman	1.52	15200	239.18	1	0.0051	47112
Eloise	5.5	55000	865.46	1.4	0.0071	121764
Mount Colin	2.59	25900	407.55	0.42	0.0021	191133
Duncan et al., (2014)						
Starra 222	0.7	7000	110.15	1.3	0.0066	16689
Starra 276	1.1	11000	173.09	0.9	0.0046	37882
Starra Total	1.2	12000	188.83	1.6	0.0081	23246
Mount Elliott	1	10000	157.36	0.5	0.0025	61989
SWANN	0.4	4000	62.94	0.3	0.0015	41326
Lady Ella	1.5	15000	236.03	1.3	0.0066	35763
Ernest Henry	1.1	11000	173.09	0.5	0.0025	68188
Osborne	1.4	14000	220.30	0.8	0.0041	54240
Eloise	5.5	55000	865.46	1.4	0.0071	121764
Mount Dore	0.6	6000	94.41	0.1	0.0005	185967

Molar Cu/Au ratios calculated for Eastern Succession IOCGs are given in Table 5. Except for Eloise, Mt Dore and Mount Colin, molar Cu/Au ratios in all of the other Eastern Succession IOCGs deposits fall in the range exhibited by alkaline systems. Thus molar Cu/Au ratios are a useful parameter to infer metal source for the Cloncurry Belt IOCG deposits. They strongly suggest an alkaline igneous source.

However, the presence of molar Cu/Au ratios <5000 in Au-rich systems also indicates that epithermal enrichment occurred at a high crustal level above Eastern Succession IOCGs systems. For example, the Evening Star - Mount Freda target.

5. Summary and Conclusions

Discovery of a copper, gold, nickel and cobalt - rich tuffisite breccia pipe in two diamond drill cores (ES019 - DD001 and DD003) at Ausmex Evening Star prospect has significant implications for the Cloncurry District IOCG mineral system model and thus, for exploration strategies and target identification.

Tuffisite is a matrix supported heterolithic intrusive pyroclastic breccia that forms in hydrothermal gas/fluid streams that advance ahead of ascending columns of magma. Although similar in appearance pyroclastic tuffs (volcanic ash deposits), relationships in the core show that the lithology is intrusive in origin.

The presence of a tuffisite pipe in the Evening Star - Mount Freda prospect indicates a close proximity to the large magmatic metal source that produced epithermal high-grade gold mineralisation at Mount Freda and also in Ausmex Golden Mile exploration area.

Uniformity of rare earth profiles, over a 8.5 m wide brecciated core interval, indicates that tuffisite pipe formation involved a very-high fluid/rock ratio and efficient mixing. Chemistry of the core shows that the fluid was fluorine, tellurium and sulphur rich, allowing the transport of Au, Ag, Cu, Ni and Co etc derived from a deeper alkaline IOCG or porphyry source.

Identification of tuffisite was based initially on structure and textural relationships in the DD001 core. It was subsequently identified DD003 where it cuts crackle brecciated quartzite.

In DD001, the metal-rich tuffisitic breccia pipe is 8.5 m wide and occurs at a depth of 80 to 88.5 m. In DD003, the brecciated unit is deeper (between 159.52 and 163 m). It is also narrower in DD003 (3.48 m), suggesting that it is a plunging diatreme-like intrusion.

A 3.6 m wide interval comprising native copper bearing gossan occurs at a shallower depth in DD001 (59.5-63 m). From the core logging, this zone was provisionally interpreted to related to the tuffisite that was identified between 80 and 88.5 m

From the orientation of the core, the tuffisite pipe is inferred to plunge towards the east, in the direction of the large Canteen magnetic anomaly that Ausmex shares with Newcrest Mining Limited

This south east - north west vector is also consistent with the interpretation that the tuffisite pipe could have acted as a conduit for hydrothermal fluids that generated the gold-rich epithermal mineral system at Mount Freda. The link between the tuffisite brecciation and epithermal processes is also supported by epithermal colloform banded silica - rich veins and quartz vugs that cut units of tuffisite.

Assays from DD001 and DD003 confirm the metallogenic significance of the tuffisite breccia system.

Tuffisite breccias in DD001 and DD003 cores have significant metal contents, e.g., copper (1060 to 9640 ppm; average 8420 ± 3321 and 3290 to 21,700 (2.17%) ppm; average 8530 ± 7612 ppm), gold (0.03 to 0.69 g/t; average 0.36 ± 0.18 g/t and 0.19 to 3.36 g/t; average 1.29 ± 1.79 g/t), nickel (107 to 599 ppm; average 339 ± 121 ppm and 92 to 309 ppm; average 233 ± 105 ppm), cobalt (124.5 to 496 ppm; average 295 ± 98 ppm and 82.6 to 222 ppm; average 192 ± 70 ppm) and molybdenum (3.29 to 12.7 ppm; average 6.63 ± 3.37 ppm and 3.84 to 11.1 ppm; average 5.26 ± 1.36 ppm).

The tuffisite also contains anomalous bismuth, sulphur and tellurium e.g., bismuth (0.07 to 2.52 ppm; average 0.80 ± 0.89 and 0.28 to 1.24 ppm; average 0.64 ± 0.52 ppm), sulphur (2.8 to 10 wt.%; average 8.2 ± 2.2 and 3.25 to 6.43 wt. %; average 5.6 ± 1.4 wt. %) and tellurium (3.29 to 12.7 ppm; average 6.63 ± 3.37 and 0.7 to 3 ppm; average 0.64 ± 0.52 ppm).

The native Cu and gossanous unit in DD001 exhibits similar or even more extreme levels of enrichment, e.g., copper (1.03 to 4.32 wt. %; average 2.65 ± 1.37 wt. %) gold (0.33 to 2.07 g/t; average 1.08 ± 0.64 g/t), nickel (443 to 1100 ppm; average 723 ± 251 ppm), cobalt (177 to 881 ppm; average 508 ± 314 ppm) and molybdenum (8.75 to 70.4 ppm; average 32 ± 23.8 ppm). This unit also contains anomalous bismuth, sulphur and tellurium e.g., bismuth (0.43 to 1.73 ppm; average 0.93 ± 0.51 ppm), sulphur (5.7 to 10 wt.%; average 9.1 ± 1.9 wt.%) and tellurium (3.42 to 7.46 ppm; average 5.1 ± 1.7 ppm).

When compared to the mean composition of 155 assays of Soldiers Cap Group host rocks in DD001, the tuffisite and gossanous unit are clearly anomalous. For example, copper (553 ± 1075 ppm), gold (0.02 to 0.06 g/t), nickel (90 ± 114 ppm), cobalt (102 ± 135 ppm), molybdenum (2.26 ± 3.14 ppm), bismuth (0.11 ± 0.22 ppm), sulphur (1.14 ± 2.33 wt.%) and tellurium (0.29 ± 0.62 ppm).

Other key findings are as follows;

(1) The elements association (Cu - Co - Ni - Au with Sc and Te) in the tuffisite and Cu-rich gossan at Evening Star indicates derivation of the mineral system from an

ultramafic - mafic source. The discovery of Fe-rich pyroxenite dykes in ES19DD001 and ES19DD003 core provides a link with this mantle source.

(2) Molar Cu/Au ratios <100,000 are also consistent with derivation of metals from an alkaline ultramafic (plume), possible porphyry metal source, as suggested by Collerson (2019).

(3) Pyroxenites, carbonate-rich mela-gabbros and alkali syenites, possibly associated with carbonatite, are present as dykes. The dykes have discordant contacts to fabrics in the host quartzites and have apophyses that cut the country rock fabrics at a high angle. These discordant relationships indicate that emplacement of the pyroxenites and mela-gabbros post-dated regional deformation associated with the Isan Orogeny at 1600 and 1580 Ma (Giles et al., 2006).

(4) Pyroxenite dykes and narrow carbonate veins are intimately associated with zones of potassium feldspar and locally magnetite, crystallisation. These lithologies are interpreted as potassic fenites. They clearly overprint and destroy metamorphic fabrics in the country rock Mount Norna Quartzite.

(5) The presence of widespread K and Fe alteration indicates a proximal relationship of these cores to the source of the metasomatizing fluids.

Pyroxenites, carbonate-rich mela-gabbros and alkali syenites possibly associated with carbonatite occur as dykes in diamond drill core (ES019 - DD001 and DD003) at Ausmex Evening Star tenement. This tenement is located above the western and north western extension of the magnetic anomaly at the Canteen IOCG exploration target shown in Figure 2.

The dykes have discordant contacts to fabrics in the host quartzites and have apophyses that cut the country rock fabrics at a high angle. These relationships indicate that emplacement of the pyroxenite dykes and mela-gabbros post-dated regional deformation associated with the Isan Orogeny between 1600 and 1580 Ma (Giles et al., 2006).

The pyroxenite dykes and narrow veins of carbonate are invariably associated with zones of potassium feldspar alteration that are interpreted as potassic fenites.

These metasomatic fenite zones clearly overprint and destroy metamorphic fabrics in the Mount Norna Quartzite. That these textures are similar to textures reported from South Australian IOCGs at Prominent Hill (e.g., Schlegel and Heinrich, 2015; Schlegel et al., 2018).

The widespread K and Fe alteration indicates a proximal relationship to the source of the metasomatising fluids.

Based on these observations, the magnetic anomaly is provisionally interpreted to be a volatile-rich post-tectonic alkaline ultramafic to mafic intrusion that is capped by a metal-rich epithermal system.

This epithermal system crops out along the Golden Mile, between Evening Star and Gilded Rose. The presence of this Au-rich zone reflects mineral deposition at a shallow crustal depth (<1,000 m) from magmatically derived hot-spring fluids that emanated from a deeper igneous source.

A zone of sulphide-rich and carbonate-rich tuffisite identified at different depths in ES019 - DD001 and DD003 is important in this regard. Tuffisitic lithologies are common in alkaline complexes (Rosatelli et al., 2010), and also in hydrothermal systems (Williams et al., 2000). **Thus, the tuffisites could represent pipe-like brecciated conduits that served as a channels for epithermal fluid and metal transport. This could have significant implications for exploration.**

Volatile-rich post-tectonic alkaline ultramafic to mafic intrusions provide an appropriate source of the poly-metallic element association reported from the IOCG mineral systems in the Cloncurry District.

The presence of pyroxenite explains the elevated Sc values reported from the Mt Freda - Evening Star mineral system, because pyroxene is a mineral that accommodates Sc into its crystal structure.

These reconnaissance observations have significant implications for better understanding the Cloncurry Belt IOCG mineral system and hence, the IOCG prospectivity of the area, thus the exploration strategy for Ausmex.

6. Recommendations

To better constrain the mineral system and hence improve exploration targeting, it is recommended that a litho-geochemical study be undertaken on ~ 50 selected lithologies from (ES019 - DD001 and DD003).

Suitable samples were identified during the site visit which formed the basis for this report.

The work would involve:

- Preparation of polished thin sections for petrographic examination and SEM mineral chemical documentation.
- Identifying and describing the petrography of each sample.
- Undertaking a LA-ICPMS geochronological study of titanite to constrain the age of the mineral system.
- Major and trace element analysis of each sample, including F analysis and Au-Pt-Pd assays.

A proposal for this work can be provided if requested.

7. References Cited

- Aleinikoff, J.N., Slack, J.F., Lund, K., Evans, K.V., Fanning, C.M., Mazdab, F.K., Wooden, J.L., Pillers, R.M., (2012) Constraints on the timing of Co-Cu+Au mineralization in the Blackbird district, Idaho, using SHRIMP U-Pb ages of monazite and xenotime plus zircon ages of related Mesoproterozoic orthogneisses and metasedimentary rocks. *Econ. Geol.* 107: 1143–1175.
- Aleinikoff, J.N., Lund, K., Fanning, M.C., (2015) SHRIMP U-Pb and REE data pertaining to the origins of xenotime in Belt Supergroup rocks: evidence for ages of deposition, hydrothermal alteration, and metamorphism. *Can. J. Earth Sci.* 52: 722–745.
- Anders, E., Grevesse, N. (1989) Abundances of the elements: Meteoritic and solar. *Geochim. Cosmochimica Acta* 53: 197-214.
- Bau M. (1996) Controls on the fractionation of isovalent trace elements in magmatic and aqueous systems: Evidence from Y/Ho, Zr/Hf, and lanthanide tetrad effect. *Contrib. Mineral. Petrol.* 123: 323-333.
- Bau, M., Dulski, P. (1995) Comparative study of yttrium and rare-earth element behaviours in fluorine-rich hydrothermal fluids. *Contrib. Mineral. Petrol.* 119: 213-223.
- Betts, P.G., Giles, D., Schaefer, B.F., Mark, G., (2007) 1600–1500 Ma hotspot track in eastern Australia: Implications for Mesoproterozoic continental reconstructions: *Terra Nova*, 19: 496–501.
- Betts, P.G., Giles, D., Foden, J., Schaefer, B.F., Mark, G., Pankhurst, M.J., Forbes, C.J., Chalmer, N.C., Hills, Q., (2009) Mesoproterozoic plume-modified orogenesis in eastern Precambrian Australia: *Tectonics*, 28: 1–28.
- Brugger, J., Liu, W., Etschmann, B., Mei, Y., Sherman, D.M., Testemale, D.S. (2016) A review of the coordination chemistry of hydrothermal systems, or do coordination changes make ore deposits? *Chemical Geology*, 447: 219-253.
- Buhn, B. (2008) The role of the volatile phase for REE and Y fractionation in low-silica carbonate magmas: implications from natural carbonatites, Namibia. *Mineral. Petrol.* 92: 453 - 470.
- Cherry, A.R., Ehrig, K., Kamenetsky, V.S., McPhie, J., Crowley, J.L., Kamenetsky, M.B. (2018) Precise geochronological constraints on the origin, setting and incorporation of ca. 1.59 Ga surficial facies into the Olympic Dam Beccia Complex, South Australia. *Precamb. Res.* 315: 162-178.
- Collerson, K D, Lal, J, Williams, Q and Rost, S, (2015) Cracking the metallogenic code for Fijian epithermal gold mineralisation. AusIMM Pacrim Conference Ext. Abstract March 2015, 219-226.
- Collerson K. D., (2019) Cobalt and HREE Mineral Systems in the Mount Isa Block. Report for GSQ
https://qdexguest.dnrm.qld.gov.au/portal/site/qdex/search?REPORT_ID=111110&COLLECTION_ID=999.
- Cox, D.P. & Singer, D.A. (1988) Distribution of gold in porphyry copper deposits, *U.S. Geological Survey Open File Report* 88-46.
- Duncan, R.J., Stein, H.J., Evans, K.A., Hitzman, M.W., Nelson, E.P., Kirwin, D.J., (2011) A new geochronological framework for mineralization and alteration in the Selwyn-Mount Dore corridor, Eastern fold belt, Mount Isa Inlier, Australia: Genetic implications for iron oxide copper-gold deposits: *Econ. Geol.*, 106: 169–192.

- Duncan, R.J., Hitzman, M.W., Nelson, E.P., Togtokhbayar, O. (2014) Structural and lithological controls on iron oxide copper-gold deposits of the Southern Selwyn-Mount Dore corridor, Eastern fold belt, Queensland, Australia: *Econ. Geol.*, 109: 419–456.
- Elliott, H.A.L., Wall, F., Chakhmouradian, A.R., Siegfried, P., Dahlgren, S., Weatherley, S., Finch, A.A., Marks, M.A.W., Dowmen, F., Deady, E. (2018) Fenites associated with carbonatite complexes: A review. *Ore Geol. Rev.* 93: 38-59.
- Giles, D., Betts, P., Ailleres, L., Hulscher, B., Hough, M., Lister, G. (2006) Evolution of the Isan Orogeny at the southeastern margin of the Mt Isa Inlier. *Aust. J. Earth Sci.* 53: 91-108.
- Groves, D., Vielreicher, N.M., (2001) The Phalabowra (Palabora) carbonatite-hosted magnetite-copper sulfide deposit, South Africa: an end-member of the iron-oxide copper-gold-rare earth element deposit group? *Mineralium Deposita* 36: 189-194.
- Heinrich, C.A., Günther, D., Audétat, A., Ulrich, T. & Frischknecht, R. (1999) Metal fractionation between magmatic brine and vapor, determined by microanalysis of fluid inclusions. *Geology*, 27: 755–758.
- Heinrich, C.A., Halter, W.E., Landtwing, M.R., Pettke, T. (2005) The formation of economic porphyry copper (- gold) deposits: constraints from microanalysis of fluid and melt inclusions. *Geol. Soc. Lond. Spec. Publ.* 248: 247 - 263.
- Jagodzinski, E.A., (2014) The age of magmatic and hydrothermal zircon at Olympic Dam, Australian Earth Sciences Convention, Volume 110. Geological Society of Australia Abstracts, Newcastle, Australia, pp. 260.
- Jagodzinski, E.A., Reid, A., Crowley, J., McAvaney, S.O., Wade, C., (2016) Precise zircon U-Pb dating of a Mesoproterozoic Silicic Large Igneous Province: the Gawler Range Volcanics and Benagerie Volcanic Suite, South Australia, Australian Earth Sciences Convention, Volume 118. Geological Society of Australia, Adelaide, Australia, pp.494.
- Kesler, S.E. (1973) Copper, molybdenum and gold abundances in porphyry copper deposits. *Econ. Geol.* 68: 106 - 112.
- Kessel, R., Schmidt, M.W., Ulmer, P., Pettke, T. (2005) Trace element signature of subduction-zone fluids, melts and supercritical liquids at 120-180 km depth. *Nature*, 437:724-727.
- Landis, G.P., Hofstra, A.H. (2012) Ore genesis constraints on the Idaho Cobalt Belt from fluid inclusion gas, noble gas isotope and ion ratio analyses. *Econ. Geol.* 107:1189-1205.
- Liu, W., Borg, S.J., Testemale, D., Etschmann, B., Hazemann, J.-L., Brugger, J. (2011) Speciation and thermodynamic properties for cobalt chloride complexes in hydrothermal fluids at 35–440°C and 600 bar: An in-situ XAS study. *Geochim. Cosmochim. Acta*, 75: 1227-1248.
- Loubet, M., Bernat, M., Javoy, M., Allegre, C.J., (1972) Rare earth contents in carbonatites. *Earth Planet. Sci. Lett.* 14: 226-232.
- McDonough, W. F., Sun S.-S. (1995) The composition of the Earth. *Chem. Geol.*, 120: 223–253.
- Mitchell, R.H. (2005) Carbonatites, carbonatites and carbonatites. *Canadian Mineralogist*, 43: 2049-2068.
- Muller, D., Groves, D.I. (2018) Potassic Igneous Rocks and Associated Gold Copper Mineralisation. Springer, 398 pp.

- Murakami, H., Jung Hun Seo, J.H. & Heinrich, C.A. (2010) The relation between Cu/Au ratio and formation depth of porphyry-style Cu–Au ± Mo deposits. *Miner. Deposita*. 45: 11-21.
- Oliver, N.H.S., Holcombe, R.J., Hill, E.J., Pearson, P.J. (1991) Tectono-metamorphic evolution of the Mary Kathleen Fold Belt, Northwest Queensland - a reflection of mantle plume processes. *Australian Journal of Earth Sciences* 38: 425-455.
- Porter, T.M. (2016) The geology, structure and mineralisation of the Oyu Tolgoi porphyry copper-gold-molybdenum deposits, Mongolia: A review. *Geoscience Frontiers* 7: 375-407.
- Rosatelli, G., Wall, F., Stoppa, F., Brilli, M. (2010) Geochemical distinctions between igneous carbonate, calcite cements, and limestone xenoliths (Polino carbonatite, Italy): spatially resolved LAICPMS analyses. *Contrib. Mineral. Petrol.* 160: 645-661.
- Saintilan, N.J., Creaser, R.E., Bookstrom, A.A. (2017) Re-Os systematics and geochemistry of cobaltite (CoAsS) in the Idaho cobalt belt, Belt-Purcell Basin, USA: Evidence for middle Mesoproterozoic sediment-hosted Co-Cu sulfide mineralization with Grenvillian and Cretaceous remobilization. *Ore Geol. Rev.*, 86: 509-525.
- Schlegel, T.U., Heinrich, C.A., (2015) Alteration and lithology control Cu mineralization at Prominent Hill iron-oxide copper-gold deposit, Gawler craton, South Australia. *Econ. Geol.* 110, 1953–1994.
- Schlegel, T.U., Wagner, T., Boyce, A., Heinrich, C.A., (2017) A magmatic source of hydrothermal sulfur for the Prominent Hill deposit and associated prospects in the Olympic iron oxide copper-gold (IOCG) province of South Australia. *Ore Geol. Rev.*, 89: 1058-1090.
- Schlegel, T.U., Wagner, T., Wallem M., Heinrich, C.A., (2018) Hematite Breccia-Hosted Iron Oxide Copper-Gold Deposits Require Magmatic Fluid Components Exposed to Atmospheric Oxidation: Evidence from Prominent Hill, Gawler Craton, South Australia. *Econ Geol.* 113: 597-644.
- Seward T. M., Barnes H. L. (1997) Metal transport by hydrothermal ore fluids. In *Geochemistry of Hydrothermal Ore Deposits* (ed. H. L. Barnes). John Wiley & Sons.
- Sinclair, A. J., Drummond, A.D., Cater, N.C. & Dawson, K.M. (1982) A preliminary analysis of gold and silver grades of porphyry-type deposits in western Canada. In: Levinson, A. A. (ed) *Precious metals in the Northern Cordillera. Association of Exploration Geochemists*, Rexdale, pp 157 – 172.
- Singer, D.A., Berger, V.I. & Morin, B.C. (2005) Porphyry copper deposits of the world: database, map, and grade and tonnage models. U.S. Geological Survey Open File Report 2005-1060.
- Spandler, C., Hammerli, J., Sha, P., Hilbert-Wolf, H., Hu, Y., Roberts, E., Schmitz, M. (2016) MKED1: A new titanite standard for in situ analysis of Sm-Nd isotopes and U-Pb geochronology. *Chem. Geol.* 425: 110-126.
- Sillitoe, R.H. (1997) Characteristics and controls of the largest porphyry copper–gold and epithermal gold deposits in the circum-Pacific region. *Aust. J. Earth Sci.* 44: 373–388.
- Taylor, S.R. & McLelland, S.M. (1985) The continental crust; Its composition and evolution. Blackwell Scientific Publishers, Oxford, 312 pp.
- Tooth, B., Brugger, J., Ciobana, C. Liu, W. (2008) Modeling of gold scavenging by bismuth melts coexisting with hydrothermal fluids. *Geology*, 36: 815-818.

- Williams-Jones, A.E., Vasyukova, O.V. (2018) The economic geology of scandium, the runt of the rare earth element litter. *Econ. Geol.* 113: 973-988.
- Williams, C.L., Thompson, T.B., Powell, J.L., Dunbar, W.W. (2000) Gold-Bearing Breccias of the Rain Mine, Carlin Trend, Nevada. *Econ. Geol.* 95: 391-404.

8. Peer Review

Reviewed by Emeritus Professor S. Golding, School of Earth and Environmental Sciences, The University of Queensland.

9. Certificate of Qualified Person

I, Emeritus Professor Kenneth D. Collerson, am the Principal of KDC Consulting (KDC²) 33 Cramond St, Wilston, 4051 Queensland, Australia.

This certificate applies to this technical report titled **Lithological and Chemical Constraints on the Mount Freda-Evening Star Mineral System, Cloncurry District Improve IOCG Metal Source Targeting** has an effective date of 25th June, 2019.

I am a Fellow of the Australasian Institute of Mining and Metallurgy (#100125). I graduated in 1993 as Doctor of Philosophy (Geology) from the University of Adelaide, South Australia and also have a Bachelor of Science degree with 1st Class Honours from University of New England, N.S.W., Australia (awarded in 1997). Emeritus Professorial status at the University of Queensland acknowledges of my contribution to research, management and teaching in the University sector.

I have practiced my profession as a Principal Consultant with Salva Resources, HDR Salva and Caracle Creek (Toronto) and as a self-employed consultant for more than 35 years. As a Principal Consultant in mineral exploration I have an excellent record of discovery. I have worked on a variety of multi-commodity metals exploration projects through high-level consulting activities in more than 15 countries.

In a consultancy for Geological Survey of Queensland (2014-2016) using spinifex grass as a biogeochemical exploration medium in the Simpson Desert, in 2014 I discovered a Devonian age alkaline metallogenic province, (Diamantina Province). Importantly, I showed that the Diamantina Province is part of a much larger belt (a plume track) of ~ 440 Ma to 365 Ma igneous activity that extends more than 2000 km from central NSW to the Northern Territory. The entire belt is prospective for a range of metals including scandium, cobalt, PGEs, copper, and gold, as well as for diamond.

Recent industry consultancies include:

- AusMex Ltd September 2018 -Rare Earth Element - Cobalt-Copper-Gold Mineral System at Burra, S.A: Significance of the AusLAMP Magnetotelluric Anomaly
- Hammer Metals August 2018 - U-Pb Titanite Geochronological Constraints on Origin and Age of the Mount Philip Breccia
- Northern Cobalt June 2018 - Review of Wollongorang Project Chemistry: Mineral System and Exploration Vectors.
- Longford Resources Feb. 2018 - present. Targeting Co and PGE mineralisation in the Goodsprings area, Nevada.
- Hammer Metals Feb. 2018 - present. Identification of key mineralisation geochemical vectors, as well as mineralisation and alteration styles in the Mary Kathleen Belt
- Encounter Resources May 2017 - present. Spinifex biogeochemistry proof of concept survey over gold and Co anomalies in the Telfer area, WA
- Laconia Resources Ltd May 2017 - present. Au-Ni-PGE target generation in the Kraaipan Greenstone Belt, Botswana
- Caracle Creek International 2016 - present. Associate Pegmatite Specialist Providing field geological, petrological and geochemical advice for international clients on exploration for LCT pegmatites

- Tyranna Resources June 2016 - present. Improved understanding of calcrete gold geochemistry in the western Gawler Craton that allowed discrimination between true and false calcrete Au anomalies with great success.
- Macarthur Lithium 2016. Provided field geological, petrological and geochemical advice to the MD on lithium exploration in the Pilbara and Yilgarn Cratons. Developed a technique using trace elements in K-feldspar to identify the Li content of the source pegmatite. This IP has global application.
- Impact Minerals Ltd 2015 - present. Petrology and geochemistry of outcrop and drill core samples from Red Hill and Mulga Springs-Moorkaie Intrusions at Broken Hill. Decoded the geochemistry and petrology of PGE-Au-Cu-Ni-Zn mineralisation at Broken Hill, resulting in enhanced understanding of the entire mineral system at Broken Hill, one of Earth's largest accumulations of metals.
- Providence Natural Resources 2012 - present. LCT pegmatite exploration for lithium at Järkvissle in Central Sweden. Currently contracted to find a JV Partner for a JORC Li resource.
- Exco/Copper Chem 2014. Preparation of a geological briefing paper for the Mary Kathleen rare earth Government tender bid.
- Exco 2014. Preparation of a prospectivity assessment for the White Dam area, South Australia, specifically identifying geochemical vectors that allowed improved understanding of the style of mineralisation.
- Chinalco Yunnan Copper Resources Limited 2013 - April 2014. Reviewed and reinterpreted drill core at Elaine and Blue Caesar and developed new model for Cu-Au-Co-REE-U mineralisation in the Mary Kathleen Belt, NW Queensland. I identified the alkaline igneous source of metals in the terrane and demonstrated that these ~1526 Ma alkaline intrusions were emplaced at a shallow crustal depth and produced epithermal mineralisation. As well as improving knowledge of Mary Kathleen Belt mineral systems, this discovery also explains Cloncurry Belt IOCG mineralisation.
- Viti Mining Pty Ltd. 2013 April - Present. Confirmed the existence of world-class very high-grade Mn mineralisation (DSO) at a number of locations on Viti Levu, Fiji. Showed that mineralisation was hydrothermal and occurred as part of an epithermal alteration system above Au-Ag-Cu bearing shoshonite intrusions
- Golden Island Resources Pty Ltd. 2013 April - Present. Undertook a literature review and discovered "lost" reports showing very widely distributed high grade Au and Ag assays (up to 35 g/t) on Waya and Wayasewa. Showed that these islands formed an extension of the shoshonite – gold trend west of Viti Levu, and following recovery of excellent panned concentrate results the islands are now being investigated using soil geochemistry to delineate drill targets.
- Golden Island Resources Pty Ltd. 2013 April - Present. I reprocessed magnetic and gravity data for Viti Levu and discovered a previously unknown ~40 km diameter Au-bearing shoshonite caldera south of Tavua caldera that has never been drilled. The Tavua caldera is host for the >1MOz epithermal Au-Ag Emperor goldmine on Viti Levu.
- Waratah Resources 2012 December. Prospectivity assessment of Gabon and the Republic of the Congo. Reviewed the geochemistry of BIFs in Waratah Resources tenements in Gabon and the Republic of the Congo to facilitate regional exploration and resource estimation.
- ASERA Iron Project 2012. December Geochemical evaluation of Lake Vättern orthomagmatic Fe-Ti-V project, Southern Sweden. Concluded that mineralisation is hosted by an anorogenic anorthosite intrusion not IOCG as previously believed.
- Triton Gold 2012 – August to December. Geochemical interpretation, Au and Mn target assessment on Viti Levu.
- Pacific Wildcat Resources 2011 – July to October. Fieldwork in Kenya and interpretation of DD core from Mrima Hill carbonatite and outcrops of nepheline syenite in a nearby intrusion. Showed that carbonatites and syenites were genetically related forming part of

a >10 km diameter intrusion. Discovered an untested mineral system and identified zones of rare earth mineralisation for a subsequent RC and DD drilling program.

I am responsible for all sections of this draft report and am independent of the Department of Natural Resources and Mines as is described by Section 1.5 of NI 43-101.

I am confident that this report has been prepared in compliance with the JORC 2012 Code and with the instrument NI 43-101.

As of the effective date of the technical report, to the best of my knowledge, information and interpretation in the report contains all scientific and technical details that are required to be disclosed.

Dated 25th June, 2019

A handwritten signature in black ink, appearing to read 'K. Collerson', with a horizontal line extending from the end.

Professor Kenneth D. Collerson

Ph.D., FAusIMM